

Sea Level Rise and Implications for Low-Lying Islands, Coasts and Communities Supplementary Material

Coordinating Lead Authors:

Michael Oppenheimer (USA), Bruce Glavovic (New Zealand)

Lead Authors:

Jochen Hinkel (Germany), Roderik van de Wal (Netherlands), Alexandre K. Magnan (France), Amro Abd-Elgawad (Egypt), Rongshuo Cai (China), Miguel Cifuentes-Jara (Costa Rica), Robert M. DeConto (USA), Tuhin Ghosh (India), John Hay (Cook Islands), Federico Isla (Argentina), Ben Marzeion (Germany), Benoit Meyssignac (France), Zita Sebesvari (Hungary/Germany)

Contributing Authors:

Robbert Biesbroek (Netherlands), Maya K. Buchanan (USA), Ricardo Safra de Campos (UK), Gonéri Le Cozannet (France), Catia Domingues (Australia), Sönke Dangendorf (Germany), Petra Döll (Germany), Virginie K.E. Duvat (France), Tamsin Edwards (UK), Alexey Ekaykin (Russian Federation), Donald Forbes (Canada), James Ford (UK/Canada), Miguel D. Fortes (Philippines), Thomas Frederikse (Netherlands), Jean-Pierre Gattuso (France), Robert Kopp (USA), Erwin Lambert (Netherlands), Judy Lawrence (New Zealand), Andrew Mackintosh (Australia/New Zealand), Angélique Melet (France), Elizabeth McLeod (USA), Mark Merrifield (USA), Siddharth Narayan (USA), Robert J. Nicholls (UK), Fabrice Renaud (UK), Jonathan Simm (UK), AJ Smit (South Africa), Catherine Sutherland (South Africa), Nguyen Minh Tu (Vietnam), Jon Woodruff (USA), Poh Poh Wong (Singapore), Siyuan Xian (USA)

Review Editors:

Ayako Abe-Ouchi (Japan), Kapil Gupta (India), Joy Pereira (Malaysia)

Chapter Scientist:

Maya K. Buchanan (USA)

This chapter supplementary material should be cited as:

Oppenheimer, M., B.C. Glavovic, J. Hinkel, R. van de Wal, A.K. Magnan, A. Abd-Elgawad, R. Cai, M. Cifuentes-Jara, R.M. DeConto, T. Ghosh, J. Hay, F. Isla, B. Marzeion, B. Meyssignac, and Z. Sebesvari, 2019: Sea Level Rise and Implications for Low-Lying Islands, Coasts and Communities Supplementary Material. In: *IPCC Special Report on the Ocean and Cryosphere in a Changing Climate* [H.-O. Pörtner, D.C. Roberts, V. Masson-Delmotte, P. Zhai, M. Tignor, E. Poloczanska, K. Mintenbeck, A. Alegria, M. Nicolai, A. Okem, J. Petzold, B. Rama, N.M. Weyer (eds.)]. In press.

Table of contents

SM4.1	Sea Level in the Geological Past	4SM-3
SM4.1.1	Mid-Pliocene Warm Period	4SM-3
SM4.1.2	Last Interglacial	4SM-4
SM4.2	SROCC Extreme Water Level Data	4SM-5
SM4.3	Risks of Impact Assessment	4SM-6
SM4.3.1	Overview of the Methodological Protocol	4SM-6
SM4.3.2	Metrics	4SM-6
SM4.3.3	Scenarios for the Future	4SM-7
SM4.3.4	Metrics Scoring According to Their Contribution to Risk, for the Present Day and in the Future	4SM-8
SM4.3.5	Aggregated Scores per Geography, Sea Level Rise Scenario and Adaptation Scenario	4SM-9
SM4.3.6	Case Study Examples	4SM-10
SM4.3.7	Final Results	4SM-10
SM4.3.8	Rationale for Scoring per Geography	4SM-10
References	4SM-22

SM4.1 Sea Level in the Geological Past

Here, additional background related to Section 4.2.2 is provided on the recent advances and ongoing difficulties in relating changes in Global Mean Sea Level (GMSL) during the mid-Pliocene Warm Period (mPWP) and Last Interglacial (LIG) to global mean temperature and ice-sheet sensitivity.

SM4.1.1 Mid-Pliocene Warm Period

The mid-Pliocene Warm Period (mPWP) is far beyond the limit of ice cores, but various techniques have been developed to reconstruct Pliocene carbon dioxide (CO₂) concentrations from sediment archives. Geochemically based estimates published since the IPCC 5th Assessment Report (AR5) (Badger et al., 2013; Martínez-Botí et al., 2015) range from 250 to 450 ppmv (parts per million by volume), with central estimates (300–400 ppmv) similar to or slightly lower than current levels. Consistency between different and independent geochemical techniques (stable carbon isotopes of algal alkenones) (Zhang et al., 2013) and the boron isotopic composition of planktic foraminifera (Martínez-Botí et al., 2015) and inverse modelling techniques relating CO₂ changes to ocean temperature and ice volume (Stap et al., 2016), support the assessment of AR5 (Masson-Delmotte et al., 2013) that mPWP CO₂ concentrations were 300–450 ppmv. Some estimates based on the stomata of fossil leaves and needles (Hu et al., 2015; Wang et al., 2015) find evidence for values below 300 ppmv, but with considerable uncertainty. Despite these relatively modest CO₂ concentrations, mid-Pliocene global mean temperature peaked between 2°C to 4°C above pre-industrial (Haywood et al., 2016), in part due to the long timescales allowing the Earth system to approach equilibrium with the elevated radiative forcing. Seasonal temperatures and precipitation during the mPWP are deemed analogous to a Representative Concentration Pathway (RCP)4.5 future climate state beyond 2040 (Burke et al., 2018). However, the strength of polar amplification during the mid-Pliocene and magnitude, timing and duration of orbitally paced atmospheric and oceanic warming, important for evaluating the sensitivity of the Greenland and Antarctica Ice Sheets (GIS; AIS), remain uncertain (Haywood et al., 2016; Dolan et al., 2018).

Most sea level estimates for the mPWP period are considerably higher than at present. A recent compilation by Dutton et al. (2015a) argues that GMSL was at least 6 m higher, but with few constraints on the maximum. AR5 (Masson-Delmotte et al., 2013) assessed the maximum to be 14 m, with *high confidence* that it did not exceed 20 m. Post depositional processes influencing palaeo-shoreline reconstructions, including glacio-isostatic adjustment (GIA) (Raymo et al., 2011) and dynamic topography, the vertical movement of the Earth's surface in response to mantle dynamics, continue to produce considerable uncertainty in Pliocene sea level reconstructions. GMSL <20 m higher than today appear the most consistent with data corrected for GIA and dynamic topography (Rovere et al., 2014), however higher estimates exist. For example, a sea level record based on a combination of geochemical data and a water-exchange/salinity model of the Mediterranean Sea (Rohling et al., 2014) supports several tens of meters of Pliocene sea level variability and peak levels

>30 m above present sea level. These values are similar to Miller et al. (2012) who reported GMSL 22 ± 5 m (*likely* range) higher than today, based on a combination of sedimentological water depth estimates along continental margins, corrected for subsidence and loading, coral atolls, and the geochemistry of marine sediments including changes in the oxygen isotopic composition ($\delta^{18}\text{O}$) of fossil foraminiferal calcite (a record of past ocean temperature and ice volume) and trace metal ratios (used to isolate the temperature component of the $\delta^{18}\text{O}$ signal). Mid-to-late Pliocene sea level (Naish and Wilson, 2009), and Antarctic Ice Sheet (AIS) variability in particular, has been associated with 41-kyr orbital obliquity cycles (changes in the Earth's axial tilt that control the magnitude of seasonality) and ~20-kyr precession cycles (Naish et al., 2009; Patterson et al., 2014) that control the seasonal timing of perihelion (when the Earth is closest to the sun). The partitioning of Pliocene sea level changes driven by greenhouse gas forcing, orbital forcing, and internal climate system feedbacks is not exactly known (Stap et al., 2018), further complicating any direct comparisons between mid-Pliocene GMSL maxima and near-term future changes.

Since AR5, updated oxygen isotope mass balance calculations comparing the isotopic composition of the modern and Pliocene ocean (Winnick and Caves, 2015), suggest Pliocene sea level was only ~9–13.5 m above modern, with a relatively small 2–4.5 m contribution from East Antarctica in addition to West Antarctica and Greenland. However, the isotope approach relies on uncertain assumptions regarding the isotopic composition of the GIS and AIS in the warmer Pliocene (Gasson et al., 2016), and the relative contribution of ice volume versus ocean temperature in the isotopic changes. Furthermore, the technique relies on the average of multiple isotope records (Lisiecki and Raymo, 2005) with limited temporal resolution that might not represent the full range of Pliocene isotope and ice-volume variability. Additional complications come from isotope data themselves, because they could contain systematic 'diagenetic' errors that bias relationships between isotope values and sea level (Raymo et al., 2018). The apparent lack of an East Antarctic contribution to Pliocene sea level suggested by Winnick and Caves (2015) also contradicts more direct geological evidence from the Antarctic margin, recording cyclic retreat of the East Antarctic margin into the deep Wilkes subglacial basin (Cook et al., 2013; Patterson et al., 2014; Bertram et al., 2018). Subsequent work, using isotope-enabled climate and ice sheet models to constrain the isotope mass balance problem concluded that an Antarctic contribution to mid-Pliocene GMSL of 13 m is consistent with the isotope records (Gasson et al., 2016). This higher GMSL estimate implies that up to ~10 m of sea level rise (SLR) could have been contributed by East Antarctica, in better agreement with the emerging geological records from the East Antarctic margin (Cook et al., 2013; Patterson et al., 2014; Bertram et al., 2018).

Shakun et al. (2018) measured cosmogenic nuclide concentrations in Antarctic-proximal marine sediment cores and concluded that extensive East Antarctic subaerial land surfaces were not exposed during the Pliocene, implying that only marine-based ice was lost. Assuming all the marine-based ice in West Antarctica (equivalent to ~3.3 m GMSL) (Bamber et al., 2009) and East Antarctica (~19.2 m) (Fretwell et al., 2013) was vulnerable to mid-Pliocene warmth, this places an upper bound on Antarctica's potential contribution to sea

level of ~22.5 meters, with the potential for another ~7.4 m of GMSL rise from Greenland (Morlighem et al., 2017). This sums to a total of about 30 m, but only if the GIS and AIS were retreated at the same time. Koenig et al. (2014) simulated the GIS response to Pliocene warmth and reduced Arctic sea ice and found near complete loss of the ice sheet, equivalent to 5.8 m GMSL rise, is possible. An ice sheet modelling study including both the GIS and AIS from de Boer et al. (2017b) yields a maximum combined ice sheet contribution to Pliocene sea level of 13.3 m. Their results show that the ice sheets in Greenland and Antarctica responded out of phase as a consequence of precessional orbital forcing (Raymo et al., 2006). The anti-phasing of Northern versus Southern Hemispheric ice sheets (de Boer et al., 2017a) is an important emerging issue, because the expansion of ice in one hemisphere during a mid-Pliocene sea level high stand consequently requires a larger proportional contribution to GMSL rise from the other hemisphere. Orbital anti-phasing of ice volume on Antarctica and Greenland also reduces the maximum potential GMSL rise. For example, assuming the GIS was comparable to its modern state while marine-based in Antarctica was fully retreated would result in no more than ~23 m of GMSL rise.

Recent ice sheet modelling studies of mid-Pliocene ice loss on Antarctica (Austermann et al., 2015; Yamane et al., 2015; DeConto and Pollard, 2016) range widely, between 5.4 and 17.8 m sea level equivalent. A model intercomparison study (de Boer et al., 2015) indicated that the largest uncertainty in modelling the mPWP is related to the mass balance forcing of AIS models. Subsequently, an ice sheet model including new, but uncertain parameterisations of glaciological processes, including the influence of surface meltwater on crevasse penetration and ice shelf collapse, and calving of marine-terminating ice cliffs (marine ice cliff instability (MICI); see Cross-Chapter Box 8 in Chapter 3) demonstrates the potential for considerable Pliocene ice loss in East Antarctica, in addition to West Antarctica (Pollard et al., 2015; DeConto and Pollard, 2016). Golledge et al. (2017) demonstrated that ocean melt at grounding lines is capable of causing Pliocene ice retreat in East Antarctic basins. In this case, the model uses a sub-grid melt scheme that applies melt under partially grounded grid cells. This numerical treatment increases the model's sensitivity to ocean forcing, although the validity of the approach remains uncertain (Yu et al., 2017; Seroussi and Morlighem, 2018). Antarctic bedrock underlying the ice sheet has probably evolved since the Pliocene (Aitken et al., 2016; Colleoni et al., 2018), contributing additional uncertainty to the palaeo ice sheet simulations, but this has yet to be fully explored with ice sheet models. Given the ongoing uncertainties in mid-Pliocene sea level reconstructions, the wide range of ice sheet model results, and unknown partitioning of greenhouse gas versus orbital forcing of ice sheet loss, there is *low confidence* in mPWP sea level as a guide for future sea level or for quantitative validation of ice sheet models.

SM4.1.2 Last Interglacial

Global mean temperatures during the LIG were not as warm as the mPWP and only slightly warmer (0.5°C–1.0°C) than pre-industrial (Capron et al., 2014; Dutton et al., 2015a; Fischer et al., 2018). Sea surface temperatures were comparable to today (Hoffman et al.,

2017). Despite the minimal warmth relative to today's climate, GMSL was considerably higher (Kopp et al., 2009). Climate models indicate a small (0.35–0.4 m) contribution to GMSL from ocean thermal expansion during the LIG (McKay et al., 2011; Goelzer et al., 2016), implicating land ice as the dominant source of the elevated sea levels. Dutton et al. (2015a) present an updated review of Eemian sea level based on geological indicators, indicating that GMSL was 6–9 m higher than today. This is in line with the earlier probabilistic estimate of Kopp et al. (2009), based on a global compilation of GMSL data. Considerable uncertainty remains however, as demonstrated by Düsterhus et al. (2016), who applied data assimilation techniques including GIA corrections to the same LIG dataset used by Kopp et al. (2009). They found good agreement (7.5 ± 1.1 m *likely* range) with Kopp et al. (2009) and Dutton et al. (2015a), but only when certain statistical assumptions and model inputs were used. Estimates of peak LIG sea level were found to be especially sensitive to the assumed ice history before and after the LIG, as found in other studies (Lambeck et al., 2012; Dendy et al., 2017). One plausible ice history used by Düsterhus et al. (2016) increased their central estimate to 14.7 m. Austermann et al. (2017) compared a compilation of LIG shoreline indicators with dynamic topography simulations. They found that vertical surface motions driven by mantle convection can produce several meters of uncertainty in LIG sea level estimates, but their mean and most probable estimates of 6.7 m and 6.4 m are broadly in line with other studies.

The relative contributions to peak GMSL from the loss of Greenland versus Antarctic ice remains difficult to quantify from geological indicators. Kopp et al. (2009) argue for two highstands within the LIG with the first peak attributable to Antarctica; however, the shape of the LIG sea level curve continues to be contested (Rovere et al., 2016). Some field sites exhibit evidence of multiple peaks in sea level, including multiple generations of reef growth in the Seychelles, the Yucatan peninsula, and the Bahamas among other sites (Blanchon et al., 2009; Vyverberg et al., 2018), but debate remains over the interpretation of this evidence. Barlow et al. (2018) argue that a sea level oscillation of >4 m is not plausible, but they do not rule out the possibility of smaller, meter-scale oscillations within the LIG. The role of the Greenland versus Antarctic ice sheet in this variability is not known with sufficient certainty to allow an assessment.

Atmospheric modelling results remain too inconsistent to provide definitive guidance on Greenland climate during the LIG. Surface mass balance varies strongly among atmospheric models with different resolutions and surface mass balance schemes (Plach et al., 2018), and different mass balance forcings produce very different spatial patterns of GIS retreat (Colleoni et al., 2014). Proxy climate reconstructions and the magnitude of LIG summer warming over the GIS also continue to be contested (Goelzer et al., 2016). Ice cores in north-central Greenland and lake archives in northwest Greenland indicate summer temperatures >6°C warmer than pre-industrial (Landais et al., 2016; Yau et al., 2016; McFarlin et al., 2018), but this large increase in summer temperature is incompatible with limited ice retreat in ice sheet models (Dahl-Jensen et al., 2013; Landais et al., 2016; Yau et al., 2016), or ice cores and internal ice layer imaging by radar (Dahl-Jensen et al., 2013) indicating the persistent presence of an extensive GIS through the LIG. This suggests the GIS was either

insensitive to LIG temperature changes, temperatures inferred from ice core oxygen isotope records are overestimated, or they were short lived. Bierman et al. (2016) used cosmogenic ^{10}Be and ^{26}Al of marine sediments to argue that large ice caps have persisted in east Greenland during the last 7.5 Myr. Data from ^{10}Be and ^{26}Al measurements of sediments below the ice suggest extensive, episodic ice-free conditions in Greenland's interior (Schaefer et al., 2016), but the duration and frequency of such events are unknown. Whether these ice core and geological findings are compatible depends on the extent and thickness of the LIG ice sheet.

Simulations with coupled climate-ice sheet models of Greenland indicate a GIS contribution to LIG SLR of only up to 50 mm per century (Helsen et al., 2013), a total contribution to LIG sea level of as little as 0.75 m (Quiquet et al., 2013), and probably not more than 2.5 m (Helsen et al., 2013; Stone et al., 2013; Colleoni et al., 2014). In contrast, the modelling study of (Yau et al., 2016) yields a higher central estimate of 5.1 m, but with a poor fit between simulated and observed climate and surface elevation at Greenland ice core locations. While the modelling studies simulate a large range of maximum GIS retreat, they consistently indicate very little retreat early in the LIG and peak ice loss late in the interglacial around 123–122 ka (Helsen et al., 2013; Quiquet et al., 2013; Goelzer et al., 2016; Yau et al., 2016). This implies that Antarctica was the dominant contributor to the early LIG highstand that began around 129 ka (Dutton et al., 2015b), in agreement with Kopp et al. (2009), and recent ice modelling studies (DeConto and Pollard, 2016; Goelzer et al., 2016).

Antarctic ice cores and proxy sea surface temperature records in the Southern Ocean indicate $<2^\circ\text{C}$ warming in the early interglacial (Capron et al., 2014). If Antarctica was the dominant source of GMSL rise early in the LIG, this would indicate a highly sensitive AIS to relatively modest climate forcing. Subsurface ocean warming and sub-ice melt rates could have played an important role in marine-based ice loss in Antarctica (Fogwill et al., 2014; Sutter et al., 2016), but their evolution through the LIG remain virtually unknown. Additional uncertainty is driven by the lack of direct evidence of West Antarctic Ice Sheet (WAIS) retreat, and increasing recognition that maximum ice retreat in Greenland and Antarctica was controlled in part by inter-hemispheric differences in the strength of polar amplification (Stap et al., 2018) and time-evolving changes in Earth's orbit over the course of the LIG (Goelzer et al., 2016; de Boer et al., 2017a). Given these ongoing uncertainties in the relative contributions of the GIS vs AIS to GMSL as the LIG evolved, and poor constraints on local atmospheric temperatures and ice-proximal ocean conditions, an assessment of each ice sheet's sensitivity to a given climate forcing cannot be made.

GMSL high-stands during past warm periods have been used to calibrate ice sheet model physical parameters, with the models subsequently applied to future climate scenarios (DeConto and Pollard, 2016). However, relatively small differences in the assumed palaeo GMSL estimates can have a large impact on the future projections (Kopp et al., 2017; Edwards et al., 2019). Furthermore, the palaeoclimate forcing applied to the ice sheet models is itself highly uncertain. In sum, there is *low confidence* in the utility of mPWP and LIG GMSL as direct guides on future sea level or their validation of ice sheet models.

SM4.2 SROCC Extreme Water Level Data

These files contain the underlying data for the SROCC extreme water level data (Chapter 4, Figures 4.10, 4.11 and 4.12).

ant_XX: time series of the contribution of the Antarctic Ice Sheet to global mean sea level rise

Columns 05, 50, and 95 indicate the percentiles of the PDF. Values are in meters

ant_longterm_XX: contribution of the Antarctic Ice Sheet in the years 2100, 2200, and 2300

Columns 05, 50, and 95 indicate the percentiles of the PDF. Values are in meters

extremes_XX_YYYY: data on changes in extremes at each tide gauge station

Columns lon,lat: longitude and latitude in degrees. Longitude is in degrees east from the Greenwich meridian

RSL_05,50,95: percentiles of regional sea level rise in meters

AF_05,50,95: percentiles of the amplification factor (increase in the average occurrence) of the historical 1-in-100 year extreme sea level event

AF_mean: best estimate of the amplification factor, which equals the mean of the PDF

extremes_GPD_parameters: Generalized Pareto Distribution parameters for each tide gauge station

Columns lon,lat: longitude and latitude in degrees. Longitude is in degrees east from the Greenwich meridian

loc: location parameter which equals the 99th percentile of hourly values above mean sea level. Values in meters

scl_05,50,95: percentiles of the scale parameter. Values in meters

shp_05,50,95: percentiles of the shape parameter

gmsl_XX: time series of global mean sea level

Columns 05, 50, and 95 indicate the percentiles of the PDF. Values are in meters

gmsl_longterm_XX: global mean sea level in the years 2100, 2200, and 2300

Columns 05, 50, and 95 indicate the percentiles of the PDF. Values are in meters

gmsl_rate_XX: time series of the rate of global mean sea level

Columns 05, 50, and 95 indicate the percentiles of the PDF. Values are in millimeters/year

rsl_XX_YYYY.nc: NetCDF4 file with regional sea level fields

Variables x,y: longitude and latitude in degrees. Longitude is in degrees east from the Greenwich meridian

Variable slr_md: median sea level change in meters

Variables slr_he,le: standard error at the high (he) and low (le) end of the median. 5th (95th) percentiles can be found by subtracting (adding) 1.645 times the low (high) error from (to) the median. Values in meters

rsl_ts_XX.nc: NetCDF4 file with time series of regional sea level fields

Variable time: year

Variables x,y: longitude and latitude in degrees. Longitude is in degrees east from the Greenwich meridian.

Variable slr_md: median sea level change in meters

Variables slr_he,le: standard error at the high (he) and low (le) end of the median. 5th (95th) percentiles can be found by subtracting (adding) 1.645 times the low (high) error from (to) the median. Values in meters

SM4.3 Risks of Impact Assessment

SM4.3.1 Overview of the Methodological Protocol

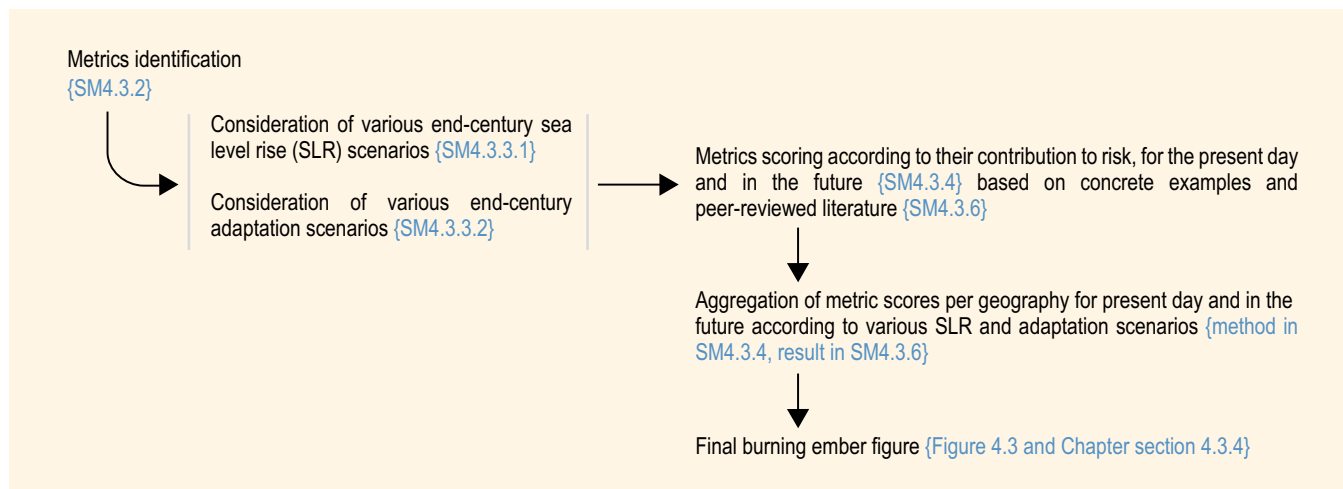


Figure SM4.1 | The general approach for building geography centred burning embers.

SM4.3.2 Metrics

Table SM4.1 below provides a synthesis of the metrics used to assess both observed impacts (present day) and projected risks (end-century).

These metrics are proxies reflecting some developments in the chapter, that is, damages to people, the built environment and land due to coastal flooding and erosion (Sections 4.3.3.2, 4.3.3.3); impacts of water resources salinisation (Section 4.3.3.4); and threats to ecosystems and ecosystem services (Section 4.3.3.5) and to human activities (4.3.3.6). More specifically, and in line with the IPCC risk

framework (Cross-Chapter Box 1 in Chapter 1) that considers risk at the crossroads of Hazards, Exposure and Vulnerability:

- Exposure and Vulnerability drivers are reflected by the density of assets (M1) and the degree of degradation of natural buffer ecosystems (M2);
- Hazards are reflected by the importance of coastal flooding (M3), coastal erosion (M4) and salinisation (M5);
- Adaptation is reflected by hard and nature-based coastal protection (M6 and M7, respectively), relocation measures (M8) and measures to limit subsidence (M9).

Table SM4.1 | Metrics used to assess risk and adaptation measures.

Metrics
<p>M1. Density of assets (population, buildings, infrastructure) – <i>Justification:</i> Section 4.3.2.2, Cross-Chapter Box 9 – <i>Scenario considered</i> for the 21st century: relatively stable density levels over the century (one scenario among others). The potential for decrease in assets density is considered through M8.</p>
<p>M2. Level of degradation of marine and terrestrial natural buffers – <i>Justification:</i> Sections 4.3.2.3 and 4.3.3.5. Natural buffers considered here are marine (coral reefs, mangroves, wetlands and sea ice; Section 4.3.3.5, 5.3) and terrestrial (beaches, dune systems and vegetation; Sections 4.3.3.3, 5.3.3) – <i>Scenario considered</i> for the 21st century: continued degradation at the same pace than recent trends.</p>
<p>M3. Relative extend of coastal flooding – <i>Justification:</i> Section 4.3.3.2</p>
<p>M4. Degree of coastal erosion (beaches and/or dune systems) or permafrost thaw – <i>Justification:</i> Section 4.3.3.3, Cross-Chapter Box 9</p>
<p>M5. Degree of salinisation of groundwater lenses, soils and surface waters – <i>Justification:</i> Section 4.3.3.4. Water resources considered here are not only for freshwater consumption, but also for agriculture, so that the impact of salinisation on aquifers have consequences on the whole resource system. Yet, sea level rise (SLR) is one of the two main controlling natural factors of aquifers volume and quality, together with precipitations; and even a low rise in sea level can have substantial effects on aquifers, especially in atoll island contexts.</p>

Metrics
<p>M6. Implementation level of adequately calibrated hard engineered coastal defences – <i>Justification:</i> Section 4.4.2.2</p>
<p>M7. Implementation level of restoration of degraded ecosystems, or creation of new natural buffers areas – <i>Justification:</i> Sections 4.4.2.2 and 4.4.2.3</p>
<p>M8. Implementation level of relocation – <i>Justification:</i> Section 4.4.2.6, Cross-Chapter Box 9. The assessment takes into consideration the specific physical constrains of each illustrative geography. In particular, while megacities and deltas have a hinterland for relocation within the territorial system, land scarcity in atoll islands implies that relocation can take place within the island if needs for relocation are moderate, but should be either in another neighbouring island or in artificially raised islands in the case of higher relocation levels. In addition, this metric refers to planned and local-scale relocation aiming at reducing the exposure of people, assets and infrastructure, and not to spontaneous relocation by individuals or small communities. This metric therefore refers to proactive managed retreat or resettlement only at a local scale, and according to the specificities of a particular context. Forced displacement and international migration are not considered in this assessment.</p>
<p>M9. Limit subsidence – <i>Justification:</i> Sections 4.4.2.2, 4.4.2.5</p>

The approach consists of assessing the potential contribution of each of these metrics to risk reduction or increase (SM4.3.4) by the end of the century, and according to various SLR and Adaptation scenarios (SM4.3.3). This assessment is based on a semi-qualitative expert judgment informed by peer-reviewed literature on real-world case studies.

SM4.3.3 Scenarios for the Future

SM4.3.3.1 Three Sea Level Rise Scenarios

In line with the specific scope of Chapter 4, this assessment focusses on the additional risks due to SLR trends and does not account for changes in extreme event climatology (waves, cyclones, etc.; Sections 4.2.3.4.1 to 4.2.3.4.3, 6.3.1.1 to 6.3.1.3). This would imply much larger risk than assessed here as, for example, this chapter however shows that events that are rare today will become more frequent in the future.

Risk transitions are located using end-century GMSL rise (thereafter, SLR, in 2100) relative to Present Day (1986–2005), and the approximate nature of these transitions was signalled in part by using the following values: 43 cm for mean SROCC RCP2.6 (range 0.29–0.59m); 84 cm for mean SROCC RCP8.5 (range 0.61–1.10m), and 110 cm for the SROCC RCP8.5 upper end of the *likely* range. See the main text for details (Table 4.3, Section 4.2.3.2).

In this exercise, GMSL serves as a representation of different possible climate change scenarios (see Panel A in Figure 4.3, Section 4.1.2). The assessment of additional risks due to SLR on specific geographies is developed not against GMSL, but against various levels of end-century relative sea level rise (RSL) in order to allow a geographically accurate approach (Panel B, Fig. 4.3). Accordingly, RSL is considered for each of the real-world case studies used for assessing risk to illustrative geographies (SM4.3.6; Table SM4.2; see coloured blocs in Panel B of Figures 4.3 and SM4.3.4), as well as in average per illustrative geographies (Table SM4.2, see coloured dotted lines in Panel B of Figures 4.3 and SM4.3.4).

N.B.: RSL includes vertical land movements, both uplift (e.g., due to tectonics) and subsidence. The causes of subsidence are both natural (e.g., tectonics, glacio-isostatic adjustment (GIA), sediment compaction) and human-induced (e.g., oil, gas and water extraction, mining activities). All of these causes are captured in RSL observations, but not in SROCC RSL projections that only include GIA and the regional gravitational, rotational and deformational responses (Section 4.2.3.4.1) to ice mass loss. Anthropogenic subsidence especially is not included in the SROCC RSL projections (Section 4.2.3.4.1): although acknowledged to be important at many locations, especially in deltas and megacities, it is challenging to project to the end of the century due to the influence of human interventions (important factor in the locations considered in this assessment). As a result, SROCC RSL projections only include the GIA component, the mass loss of glaciers and ice sheets and oceans, including their spatial patterns.

Table SM4.2 | Relative sea level rise (RSL) by 2100 at the real world case studies (italics) and per illustrative geographies. RCP is Representative Concentration Pathway, GIA is glacio-isostatic adjustment.

Location		SROCC RCP2.6	SROCC RCP8.5		GIA
		Median	Median	Upper end (>95%)	
Resource-rich coastal cities	<i>New York</i>	0.55	1.02	1.53	0.09
	<i>Rotterdam</i>	0.39	0.82	1.23	0
	<i>Shanghai</i>	0.42	0.84	1.29	-0.03
	Mean	0.45	0.89	1.35	/
Urban atoll islands	<i>South Tarawa</i>	0.49	0.92	1.32	-0.02
	<i>Funafuti</i>	0.49	0.91	1.33	-0.01
	<i>Male'</i>	0.46	0.92	1.32	-0.01
	Mean	0.48	0.92	1.32	/
Large tropical agricultural deltas	<i>Mekong</i>	0.43	0.84	1.23	-0.04
	<i>Ganges-Brahmaputra</i>	0.33	0.74	1.08	-0.04
	Mean	0.38	0.79	1.16	/
Arctic coastal communities (remote from regions of rapid GIA)	<i>Bykovskiy</i>	0.34	0.79	1.17	-0.01
	<i>Shismaref</i>	0.40	0.81	1.13	0.07
	<i>Kivalina</i>	0.37	0.77	1.10	0.06
	<i>Tuktoyaktuk</i>	0.39	0.77	1.09	0.18
	<i>Shingle Point</i>	0.40	0.76	1.10	0.17
	Mean	0.38	0.78	1.12	/

SM4.3.3.2 Two Adaptation Scenarios

Two adaptation scenarios are considered:

- (A) ‘No-to-moderate response’ (see Panel B in Figure 4.3) represents a business-as-usual scenario where no major additional adaptation efforts compared to today are implemented. That is, neither substantial intensification of current actions nor new types of actions, for example, only moderate raising of existing protections in high density areas or sporadic episodes of coastal relocation or beach nourishment where large-scale efforts are not already underway.
- (B) ‘Maximum potential response’ represents the opposite situation, that is, an ambitious combination of both incremental and transformational adaptation that leads to significant additional efforts compared to today. Examples of measures are: relocation of entire districts in a megacity or creation/restoration of beach-dune systems at a significant scale. Here, adaptation is assumed to be implemented at its full potential, that is, the extent of adaptation that is technologically possible, with minimal financial, social and political barriers.

Table SM4.3 summarises the assessment framework (and based on SM4.3.2 and SM4.3.3).

SM4.3.4 Metrics Scoring According to Their Contribution to Risk, for the Present Day and in the Future

SM4.3.4.1 Scoring Risk for the Present Day

Coastal risk gradient ranges from Undetectable to Very High (Panel A in Figure SM4.2 below). When including transitions, 7 levels are reported (Undetectable, Undetectable to Moderate, Moderate, Moderate to High, High, High to Very High, Very High) that describe a scoring scale going from 0–6, as shown in Panel B in Figure SM4.2. Based on the above mentioned semi-qualitative expert judgment, a score is attributed to each metric to reflect its contribution to current coastal risk. Positive and negative scores describe contributions to increasing or decreasing risk, respectively.

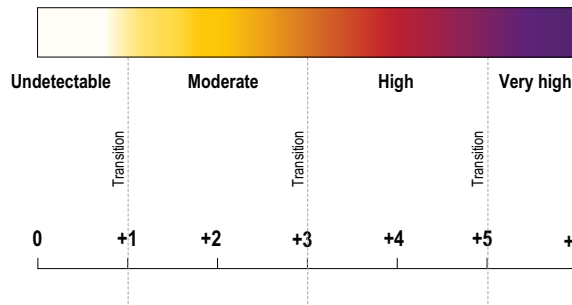
SM4.3.4.2 Scoring Coastal Risk for End-Century (Under Various Sea Level Rise and Adaptation Scenarios)

Table SM4.4 below schematically quantifies the potential additional contribution of each metric to future coastal risk (increase or reduction; positive or negative scores, respectively). Respective contributions in a 43 cm(A) scenario are compared to the Present Day (1986–2005); so that 43 cm(A) scores are additional to the Present Day ones. In the same way, and to highlight cumulative effects across SLR and Adaptation scenarios, metrics’ contributions in the 84 cm and 110 cm scenarios are compared to scores for the 43 cm and

Table SM4.3 | The assessment framework (metrics, sea level rise (SLR) scenarios, Adaptation scenarios). Red refers to SLR scenarios and Green refers to adaptation scenarios.

SLR by 2100 (compared to the Present Day, 1986–2005)	M1	M2	M3	M4	M5	M6	M7	M8	M9	Aggregated risk level
	Density of assets	Ecosystem degradation	Coastal flooding	Coastal erosion	Salinisation	Hard defences	Ecosystem restoration	Relocation	Limit subsidence	
Present Day	score	score	score	score	score	score	score	score	score	score
43 cm by end-century (A)	score	score	score	score	score	score	score	score	score	score
43 cm by end-century (B)	score	score	score	score	score	score	score	score	score	score
84 cm by end-century (A)	score	score	score	score	score	score	score	score	score	score
84 cm by end-century (B)	score	score	score	score	score	score	score	score	score	score
110 cm by end-century (A)	score	score	score	score	score	score	score	score	score	score
110 cm by end-century (B)	score	score	score	score	score	score	score	score	score	score

(a) Levels of additional risk due to climate change and sea level rise (SLR)



Inspired from IPCC SR1.5

Undetectable (white) indicates that associated impacts or risks (partly attributable to climate change and sea level rise) are not detectable.

Moderate (yellow) indicates that associated impacts or risks are detectable.

High (red) indicates severe and widespread impacts or risks.

Very high (purple) indicates very high risk of severe impacts and the presence of significant irreversibility or the persistence of climate and sea level-related hazards.

(b) Individual scores (i.e., per metric) to establish present day level of risk (per metric and geography; see SM4.3.4.1)

Figure SM4.2 | Scoring scale for assessing Present Day risk.

Table SM4.4 | Scoring methodology for assessing future risk.

Additional contribution of the metric to end-century coastal risk level	(A) No-to-moderate response	(B) Maximum potential response
No effect	[+0]	[+0]
Increases risk	[+1] Low additional contribution	[+1] Low additional contribution
	[+2] Substantial additional contribution	[+2] Substantial additional contribution
	[+3] Very substantial additional contribution	[+3] Very substantial additional contribution
Decreases risk	[-1] Low additional contribution	[-1] Low additional contribution
	[-2] Substantial additional contribution	[-2] Substantial additional contribution
	[-3] Very substantial additional contribution	[-3] Very substantial additional contribution

84 cm scenarios, respectively; so that 84 cm and 110 cm scores are additional to the 43 cm and 84 cm ones, respectively.

In parallel, the Adaptation Scenario (B) scores are most of the time based on the scenario (A) scores of the same SLR scenario. For example, the scores for 43 cm(B) describe the contribution of the implementation of adaptation measures (M6, M7, M8, M9) to the reduction of risk level at the 43 cm(A).

The scoring relies on a semi-qualitative expert judgment based on real world case studies described in peer reviewed literature. Final assessment for each geography is presented in SM4.3.7.

SM4.3.5 Aggregated Scores per Geography, Sea Level Rise Scenario and Adaptation Scenario

Figure SM4.3 builds on Figure SM4.2 to describe the equivalence between coastal risk levels (according to the IPCC frame, Panel A in Figure SM4.3) and the assessment scores per criteria (Panel B).

Four main steps for calculating future coastal risk levels are:

Step 1 For each metric, estimation of the **current contribution to coastal risk**, based on the 0–6 scale described in SM4.3.4.1 (see also Panel B in Figure SM4.3).

Step 2 Each **metric’s additional contribution to coastal risk** under various end-century SLR and Adaptation scenarios is

assessed based on the scoring scale presented in Table SM4.4. Scores for the 43 cm(A) scenario are based on Present Day (1986–2005) scores. Scores for the 84 cm(A) and 110 cm(A) scenarios are calculated based on the 43 cm(A) and 84 cm(A) scores, respectively, and in order to reflect a cumulative effect of contributions to coastal risk as sea level rises.

In parallel, the adaptation scenario (B) scores are most of the time based on the scenario (A) scores of the same SLR scenario. For example, the scores for 43 cm(B) describe the contribution of the implementation of adaptation measures (metrics M6 to M8) to the reduction of the 43 cm(A) risk level.

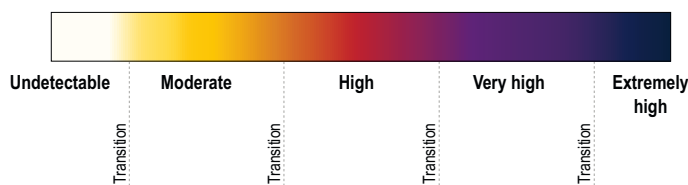
Step 3 Aggregated levels of coastal risk for the Present Day –

These risk levels result from the aggregation (i.e., addition without weighting) of the 9 metrics’ individual scores developed in Step 1. The range for Present Day (1986–2005) aggregated scores goes from 0 (i.e., undetectable contribution to risk for all metrics) to 30 (i.e., very high contribution to risk for all metrics). The equivalence in terms of risk level is based on the risk scale used in previous IPCC assessments (see panel B of Figure SM4.3).

Step 4 Aggregated levels of coastal risk for the Future –

Risk levels by the end of the century and for different SLR (A) and adaptation (B) scenarios result from the aggregation (i.e., addition without weighting) of the 9 metrics’ individual scores developed in Step 2. The range for Future aggregated scores goes from 0 to 75 (i.e., respectively undetectable and

(a) Levels of additional risk due to climate change and sea level rise (SLR)



Inspired from IPCC SR1.5
Undetectable (white) indicates that associated impacts or risks (partly attributable to climate change and sea level rise) are not detectable.

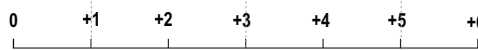
Moderate (yellow) indicates that associated impacts or risks are detectable.

High (red) indicates severe and widespread impacts or risks.

Very high (purple) indicates very high risk of severe impacts and the presence of significant irreversibility or the persistence of climate and sea level-related hazards.

Extremely high (purple-black) indicates high-end risk scenarios above which limits to adaptation could occur.

(b) Individual scores (i.e., per metric) to establish present day level of risk (per metric and geography; see SM4.3.4.1)



(c) Aggregated scores (i.e., sum of all metrics) to establish future levels of risk (combined metrics per SLR adaptation scenarios; see SM4.3.5)

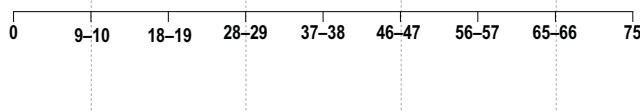


Figure SM4.3 | Scoring scale for assessing future risk.

very high contribution to risk for all metrics); this calculation is based on the combination of min/max Present Day (1986–2005) aggregated scores with additional contributions to risk for each metric (see sheet 2 in SM4.3 datafile). To consider the wide range of possible aggregated scores implies to consider situations that are already at Very High risk and where each additional cm of SLR pushes the risk level to extreme limits, that is, beyond 'Very High'. According to this, another level of risk was added to the usual IPCC risk scale, and that describes 'Extremely High' risk (see black-purple in Panel A of Figure SM4.3).

In that way, the approach is standardised among the geographies, although it is acknowledged that, for example, atolls islands and Arctic communities do not have significant (if any) space for action under M9, as well as salinisation (M5) is not an issue for megacities.

SM4.3.6 Case Study Examples

The assessment of coastal risk for each geography (resource-rich coastal cities, urban atoll islands, large tropical agricultural deltas and Arctic communities remote from regions of rapid glacio-isostatic adjustment) is based on the findings of Chapter 4 as well as on the collective expert judgment of the authors (Lead Authors and Contributing Authors). This semi-qualitative expert judgment has been informed by using, for each illustrative geography, a set of real world local case studies that have been described in the peer reviewed literature (Table SM4.5).

Scale considered:

- *Resource-rich coastal cities*: the coastal fringe
- *Urban atoll islands*: the whole island system, that is, capital islands of atoll nations
- *Large tropical agricultural deltas*: considered as a whole, and not only their coastal fringe, for three main reasons:

- SLR will contribute in some deltas (e.g., tidal deltas) in increased salinity intrusion inland, so the direct impacts will be not only on the coastal fringes;
- Some of the adaptation measures are easier if consider a whole delta system is considered: for example, basin-scale water (sediment) management (with all the inherent difficulties of course), but also in terms of retreat (migration);
- Delta level planning (e.g., the Mekong) already incorporates various delta-wide development scenarios, a couple of which are 'do not protect too much' and thus convert to saline livelihoods (aquaculture, more salt tolerant crop varieties) and preserve a freshwater environment.

- *Arctic communities*: the whole community system

See supporting material in SM4.3.8

SM4.3.7 Final Results

The SM4.3 datafile provides the full assessment database describing all the scores for each metric and each geography. The final results are reported in Table SM4.6 below.

Equivalences between final scores and risk levels as described in section SM4.3.5 and Figure SM4.4 below.

SM4.3.8 Rationale for Scoring per Geography

SM4.3.8.1 Resource-rich coastal cities

See Section 4.3.4.2.1 and Sheet 1 of the SM4.3 datafile. Main references used for the resource-rich coastal cities case study include Vellinga (2009), Delta Programme (2015), Zhou et al. (2016), Hinkel et al. (2018), Xian et al. (2018), along with those in Box 4.1.

Table SM4.5 | Real world case studies used in the assessment of current and future coastal risk. GIA is glacio-isostatic adjustment; CA, CLA and LA mean Contributing Author, Coordinating Lead Author and Lead Author, respectively.

Illustrative geography	Case studies used for background information	Main authors involved
Resource-rich coastal cities	<ul style="list-style-type: none"> – New York City (USA) – Rotterdam (The Netherlands) – Shanghai (China) <p><i>N.B.: insights from Box 4.1 have also been considered.</i></p>	<ul style="list-style-type: none"> – Maya Buchanan (USA), CA – Michael Oppenheimer (USA), CLA
Urban atoll islands	<ul style="list-style-type: none"> – Male' (Maldives) – South Tarawa main islands (Kiribati) – Funafuti (Tuvalu) 	<ul style="list-style-type: none"> – Virginie Duvat (France), CA – Alexandre Magnan (France), LA
Large tropical agricultural deltas	<ul style="list-style-type: none"> – Mekong Delta – Ganges-Brahmaputra-Meghna Delta 	<ul style="list-style-type: none"> – Fabrice Renaud (UK), CA – Zita Sebesvari (Hungary/Germany), LA
Arctic communities	<ul style="list-style-type: none"> – Bykovskiy, Russia – Shismaref, Alaska, USA – Kivalina, Alaska, USA – Tuktoyaktuk, Canada – Shingle Point, Canada <p><i>N.B.: these Arctic case studies have been selected because they are remote from regions of rapid GIA.</i></p>	<ul style="list-style-type: none"> – Donald Forbes (Canada), CA – James Ford (UK), CA

Table SM4.6 | Final aggregated levels of risk for each geography and according to various sea level rise (SLR) and Adaptation scenarios. Text in black describes the Present Day as well as the ‘No-to-moderate response’ scenarios for the future. Text in blue describes the ‘Maximum potential response’ scenarios. GIA is glacio-isostatic adjustment.

SLR by 2100 (compared to the Present Day, 1986–2005)	M1	M2	M3	M4	M5	M6	M7	M8	M9	Aggregated risk level
	Density of assets	Ecosystem degradation	Coastal flooding	Coastal erosion	Salinisation	Hard defences	Ecosystem restoration	Relocation	Limit subsidence	
Resource-rich coastal cities										
Present Day	6	1	2	1	0	-3	0	-1	0	6 – Undetectable to Moderate
43 cm (A)	7	2	4	2	0	-1	0	-1	0	13 – Moderate
43 cm (B)	6	1	1	1	0	-3	0	0	0	6 – Undetectable to Moderate
84 cm (A)	10	4	7	3	0	0	0	-2	0	22 – Moderate to High
84 cm (B)	6	1	2	1	0	-3	0	0	0	7 – Undetectable to Moderate
110 cm (A)	12	5	10	3	0	0	0	-3	0	27 – Moderate to High
110 cm (B)	8	2	4	1	0	-2	0	-1	0	12 – Moderate
Urban Atoll Islands										
Present Day	5	5	5	4	2	-2	-1	0	0	18 – Moderate
43 cm (A)	7	7	8	6	4	-2	-1	0	0	29 – Moderate to High
43 cm (B)	7	7	8	6	4	-4	-3	-3	0	22 – Moderate to High
84 cm (A)	10	9	11	8	6	-2	-1	0	0	41 – High to Very High
84 cm (B)	10	9	11	8	6	-4	0	-6	0	34 – High
110 cm (A)	13	11	14	10	8	-2	-1	0	0	53 – Very High
110 cm (B)	13	11	14	10	8	-4	0	-9	0	43 – High to Very High
Large tropical agricultural deltas										
Present Day	4	3	3	2	2	-2	-1	0	0	12 – Moderate
43 cm (A)	4	4	5	3	4	-2	-1	0	0	18 – Moderate
43 cm (B)	4	4	5	3	4	-3	-3	0	-2	14 – Moderate
84 cm (A)	4	5	8	5	6	-2	-1	0	0	26 – Moderate to High
84 cm (B)	4	5	8	5	6	-4	-2	-3	-1	19 – Moderate
110 cm (A)	4	5	11	7	8	-2	-1	0	0	33 – High
110 cm (B)	4	5	11	7	8	-5	-1	-3	0	27 – Moderate to High
Arctic coastal communities (remote from regions of rapid GIA)										
Present Day	4	5	4	5	2	-1	0	-1	0	18 – Moderate
43 cm (A)	5	7	6	8	2	-1	0	-1	0	26 – Moderate to High
43 cm (B)	5	7	6	7	2	-2	0	-2	0	23 – Moderate to High
84 cm (A)	6	10	8	11	3	-1	0	-1	0	36 – High
84 cm (B)	6	10	8	10	3	-3	0	-4	0	30 – Moderate to High
110 cm (A)	7	11	9	12	3	-1	0	-1	0	40 – High to Very High
110 cm (B)	7	11	9	11	3	-3	0	-4	0	35 – High

4SM

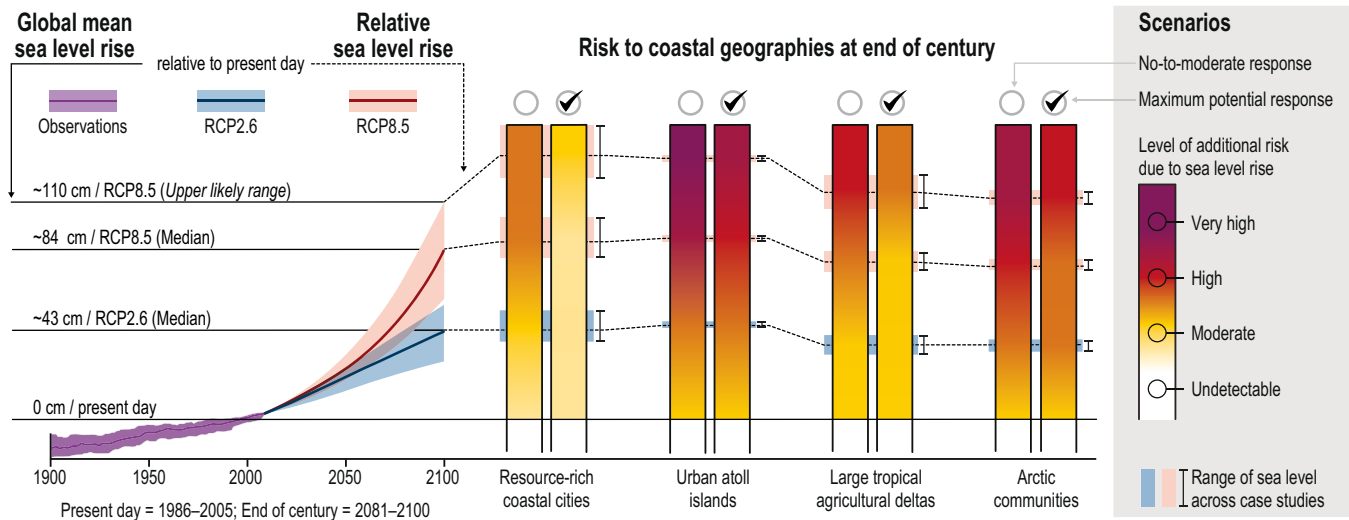


Figure SM4.4 | Additional risks from SLR on low-lying coastal geographies by the end of the 21st century (see Figure 4.3 and caption in the main text, as well as Section 4.3.4 for synthetic methodological advances and brief analysis of the results).

SM4.3.8.2 Urban Atoll Islands

See complementary information in Section 4.3.4.2.1 and Sheet 1 of the SM4.3 datafile.

The urban atoll islands considered in this analysis are the capital islands (or groups of islands) of three atoll nations in the Pacific and Indian Oceans: Fongafale (Funafuti Atoll, Tuvalu), the South Tarawa Urban District (Tarawa Atoll, Kiribati) and Male' (North Kaafu Atoll, Maldives). Atoll island countries present a quite unique situation around the world as the present and future of their populations largely depend on the responses of coral reefs to climate change and induced changes in the ocean (Hughes et al., 2017; Perry et al., 2018). As atoll islands in general, urban atoll islands have low elevation (<4 m above mean sea level) and are mainly composed of reef-derived unconsolidated material.

Urban atoll islands present a critical situation for these countries. On the one hand, they are the main economic and demographic centres at the country scale, thereby often concentrating most human assets and critical infrastructure (airports, main harbours). On the other hand, they illustrate the prominence of anthropogenic-driven disturbances to atoll island capacity to naturally adjust to ocean climate-related changes, and SLR in particular. Human disturbances affect the critical services provided by the reef-island system, in particular the coastal protection service delivered by the reef ecosystem and beach. This service consists of wave energy attenuation, which reduces wave-induced flooding and coastal erosion, and sediment provision by the reef ecosystem to the island, which is critical to island persistence over time through continuous adjustment to waves and SLR through sediment reorganisation (McLean and Kench, 2015; Quataert et al., 2015; Elliff and Silva, 2017; Storlazzi et al., 2018).

Three critical controlling factors of the future habitability of these islands are the density of assets exposed to climate-induced coastal hazards (metric M1), marine flooding (M3) and coastal erosion (M4). These critical controlling factors are interlinked with

ecosystem response to ocean-climate related pressures and the effects (detrimental or beneficial) of human activities. The following assessment takes this into consideration.

Present Day

M1: Human-driven disturbances to the natural reef-island system are inherent to high population densities and unplanned urban development. In countries such as the Maldives, Tuvalu and Kiribati, the capital atolls and island host between around a third (in the Maldives) and half (in Tuvalu and Kiribati) of the national population. This translates into high levels of population density: ~65,700 per km² in Male' (GoM-MoT 2014), ~4,200 per km² in Funafuti Atoll (McCubbin et al., 2015), ~3,200 per km² in South Tarawa (McIver et al., 2015). This all the more contributes to risk that as illustrated in Tuvalu and Kiribati, settlements concentrate on the lagoon side, that is, very low-lying (<1.80 m in elevation, e.g., South Tarawa)(Duvat, 2013) and therefore flood prone, side of islands. The capital islands also often host the main critical infrastructures of the country, especially international airports and main harbours, which are critical for the economy and more broadly the opening up to the world. Together, high population densities and the concentration of critical infrastructure in naturally low-lying areas substantially contribute to coastal risk (Duvat et al., 2013). → Final score of [5].

M2: The main ecosystems considered here are coral reefs, mangroves and sandy beaches. It is acknowledged that today, the degradation of marine and coastal ecosystems that serve as natural buffers is high in urban atoll islands due, for example, to mangrove clearing in South Tarawa (Duvat, 2013) or to human-induced coral reef degradation through land reclamation in Male' (Naylor, 2015). As a result, the above mentioned coastal protection service is most often already seriously undermined, with implications in terms of increasing coastal risk. → Final score of [5].

- M3:** High to Very High flooding risk today for all the case studies. Extreme sea levels (including during high tides) already generate flooding events on relatively large parts of islands. Experiences are reported in Male' (Wadey et al., 2017) and Funafuti (Yamano et al., 2007; McCubbin et al., 2015). Flooding is a major risk in atoll island environments as flooding events often cause substantial damages to human assets (e.g., destruction of roads, coastal protection structures and airstrips), as well as they have cascading effects on livelihoods, for example, as a result of groundwater and soil salinisation. Land scarcity in atoll environments exacerbates the importance of such damages and cascading impacts. → Final score of [5].
- M4:** Coastal erosion is already a major concern along some non-armoured shoreline sections in urban islands in South Tarawa, Kiribati (Duvat, 2013) and Fongafale, Tuvalu (Onaka et al., 2017). It is not the case in Male', Maldives, where surrounding fortifications occupy almost all the shoreline from several decades (Naylor, 2015). In urban islands, coastal erosion occurring on non-fixed shoreline sections is generally attributed to the disruption of natural processes by human disturbances, in particular land reclamation, causeway construction aimed at connecting nearby islands and sediment extraction from beaches, reef flats and shallow lagoons (Biribo and Woodroffe, 2013; Duvat, 2013; Duvat et al., 2013; Donner and Webber, 2014; McLean and Kench, 2015; Duvat, 2019). → Final score of [4].
- M5:** Salinisation already affects groundwater lenses in atoll islands, especially as a result of overwash events (Terry and Chui, 2012; Hoeke et al., 2013; Oberle et al., 2017). While the population of Male' relies on desalinated seawater, groundwater lenses still provide water for human consumption and agricultural purposes in South Tarawa, for example (Bailey et al., 2014; Post et al., 2018). This explains variable contributions of groundwater lens salinisation to risk depending on the urban atoll island considered. Despite increasing rainwater harvesting, groundwater lenses remain a primary source of domestic freshwater in South Tarawa, which advocates for their sustainable management (White and Falkland, 2010; Post et al., 2018). N.B.: attribution of groundwater lens salinisation to SLR however remain unclear (Section 4.3.3.1). Therefore, a score of [2] which reflects a moderate contribution of salinisation to risk. → Final score of [2].
- M6:** Some existing hard protection in all of the case studies. The quality of such coastal defences is however highly variable between the case studies, from appropriate engineered to poorly designed structures. Male' constitutes an exception in urbanised atoll environments as it surrounded by massive engineered structures, especially breakwaters and rock revetments (Naylor, 2015). However, although these appropriate engineered structures substantially contribute to reduce risk (i.e., individual score of -4), they don't totally eliminate the flooding hazard. At the opposite, in South Tarawa urban islands, adequate structures are seldom, with poorly designed handmade structures prevailing along the coast (Duvat, 2013; Duvat et al., 2013), therefore an individual score of [-2]. Funafuti presents a similar situation to the one of South Tarawa (Onaka et al., 2017). → Final score of [-2].
- M7:** Today, measures to protect/restore natural buffers are still limited in urban atoll contexts. A well-known example is mangrove replanting in the eastern lagoon part of South Tarawa (Donner and Webber, 2014), but such examples remain limited in the literature. → Final score of [-1].
- M8:** Today, the level of implementation of relocation measures aiming at reducing the exposure of people, assets and infrastructure remains sporadic and unplanned in urban atoll islands. Accordingly, undetectable contribution to today's coastal risk reduction was estimated. → Final score of [0].
- M9:** Not considered for urban atoll islands.
- 43(A)
- M1:** Even in the case of a relative stabilisation of the population, densities will remain high in the future (see SM4.3.2). Due to the low-lying coasts of atoll islands and the concentration of settlements along the very low-lying lagoon coast of atoll islands such as South Tarawa, even stabilised densities would translate into a substantial increase (i.e., [2] compared to Present Day) of M1 contribution to risk even under a 43 cm rise in sea level. → Final score of [2] compared to the Present Day.
- M2:** While this assessment focusses on the additional risks due to SLR, it is important to note that ocean acidification and warming will weaken the capacity of marine ecosystems, including coral reefs and mangroves, to cope with SLR (Van Hooonk et al., 2013; Pendleton et al., 2016; Perry and Morgan, 2017; Perry et al., 2018) (Sections 4.3.3.5, 5.3), which will in turn exacerbate the influence of SLR on coastal risk. → Final score of [2] compared to Present Day.
- M3:** Important increase in risk of flooding compared to today is expected (Beetham et al., 2017; Storlazzi et al., 2018). → Final score: [3] compared to Present Day.
- M4:** Coastal erosion is expected to increase substantially even under relatively small rise in sea level, mainly due to the pursuing of current trends as well as the possible increase in human-driven disturbances (e.g., sand mining) that undermine the capacity of islands to adjust to ocean-climate related pressures (McLean and Kench, 2015; Duvat, 2019). Such a role of coastal erosion in risk increase will be important in South Tarawa and Funafuti, but not in Male' where the shoreline is almost entirely fixed by engineered coastal protection structures. → Final score: [2] compared to Present Day.
- M5:** Substantial increase in risk of groundwater salinisation compared to today, as even small values of SLR are expected to significantly affect atoll islands aquifers (Bailey et al., 2016; Storlazzi et al., 2018). → Final score: [2] compared to Present Day.
- M6:** No major additional adaptation efforts compared to today. Same score as for Present Day.

M7: No major additional adaptation efforts compared to today. Same score as for Present Day. 84(A)

M8: No major additional adaptation efforts compared to today. Same score as for Present Day.

M9: Not considered for urban atoll islands.

43(B)

M1: As for 43 cm(A).

M2: As for 43 cm(A).

M3: As for 43 cm(A).

M4: As for 43 cm(A).

M5: As for 43 cm(A).

M6: Substantial additional contribution of appropriate engineered protection structures to decreasing risk, compared to business-as-usual interventions. While engineered protection structures will reduce risk of flooding especially, they will not necessarily prevent seawater infiltration due to the permeable nature of the island substratum. So even adequate coastal protection would probably not eliminate risk (Hinkel et al., 2018). → Final score: [-2] compared to 43 cm(A).

M7: In a relatively moderate increase in sea level, substantial additional contribution of ecosystem restoration efforts to decreasing risk can be expected. Despite this, human- and climate-driven disturbances of these natural buffers will not be fully removed. As a result, the Present Day natural buffering capacities of marine and coastal ecosystems cannot be fully recovered in the urban atoll island context, which prevents these ecosystems to have a very substantial contribution to risk reduction (i.e., [-3] compared to today). This reflects some irreversibility in human-driven ecosystem degradation in urban environments. → Final score: [-2] compared to 43 cm(A).

M8: Very substantial additional contribution of proactive coastal relocation (e.g., first and second lines of buildings and infrastructures; associated with relocation either on the same island or to a nearby island exhibiting medium population densities) to decreasing risk compared to business-as-usual interventions. To the point that such a relocation can compensate the extent of coastal flooding and hence the level of associated damages to the built assets. → Final score: [-3] compared to 43 cm(A).

M9: Not considered for urban atoll islands.

M1: Very substantial increased contribution to risk compared to 43 cm(A) scenario. Very substantial additional contribution of high density to risk. → Final score [3] compared to 43 cm(A).

M2: Substantial increased contribution to risk compared to 43 cm(A) scenario, due both to continued human-driven degradation of ecosystems –reminder: (A) scenarios considers no major additional adaptation efforts compared to today (SM4.3.3.2), and the impacts of ocean warming and acidification. → Final score: [2] compared to 43 cm(A).

M3: Substantial increased contribution to risk compared to 43 cm(A) scenario. This reflects the combination of very low-lying topographies with increased relative and extreme sea levels. → Final score: [3] compared to 43 cm(A).

M4: Substantial increased contribution to risk compared to 43 cm(A) scenario. Accelerated erosion at all sites due to the fact that the sediment budget of islands will already be substantially affected under a 43 cm rise in sea level, so that erosion trends continuation will result in less sediments being available at the coast in higher SLR scenarios. → Final score: [2] compared to 43 cm (A).

M5: Massive effects on the volume and quality of groundwater lenses, surface waters and soils are to be expected in a RCP8.5 scenario, therefore substantial cumulative effect in terms of contribution to risk compared to 43 cm(A). → Final score: [2] compared to 43 cm(A).

M6: No major additional adaptation efforts compared to today. Same score as for Present Day.

M7: No major additional adaptation efforts compared to today. Same score as for Present Day.

M8: No major additional adaptation efforts compared to today. Same score as for Present Day.

M9: Not considered for urban atoll islands.

84(B)

M1: As for 84cm(A).

M2: As for 84cm(A).

M3: As for 84cm(A).

M4: As for 84cm(A).

M5: As for 84cm(A).

- M6:** While the development of adequate engineered coastal defence structures will still provide some benefits in terms of risk reduction (e.g., flooding limitation, shoreline stabilisation), these protection structures will not necessarily prevent seawater infiltration due to the permeable nature of the island substratum. So even adequate coastal protection will probably not eliminate risk (Hinkel et al., 2018). As a result, and given the very low elevation and the porous nature of urban islands, one can hypothesise that higher SLR scenarios would weaken the additional benefits of coastal protection structures –although huge uncertainty remains on such a hypothesis. → Final score: [0] compared to 84 cm(B).
- M7:** No more contribution to risk reduction in higher end-century SLR: the contribution of ecosystem restoration becomes obsolete as, for example, corals will face difficulties to keep-up with SLR and mangroves will lose habitats (Sections 4.3.3.5, 5.3). As a result, a decreasing contribution to risk reduction was considered. → Final score: [-1] compared to 84 cm(A), that is [1] compared to 43 cm(B).
- M8:** More intense coastal relocation (e.g., >3 lines of buildings and infrastructures) will decrease risk, but in an atoll island context, such a level of relocation will face physical constraints due to land scarcity. To address this constraint, however, relocation to other islands in the same atoll can be envisaged (e.g., in Tarawa and Funafuti that still have many rural and uninhabited islands). In Kaafu Atoll, Maldives, where land is scarce (most islands are already settled or exploited, e.g., by resorts), additional artificially raised islands such as Hulhumale' could offer some opportunities. This highlights the potential cumulative benefits of a progressive shift in relocation approaches, from within the capital island to neighbouring or artificial islands. → Final score: [3] compared to 43 cm(B).
- M9:** Not considered for urban atoll islands.
- 110(A)
- M1:** Same justification as for M1 under 43 cm. Very substantial additional contribution of high densities compared to the 84 cm situation. → Final score: [3] compared to 84 cm(A).
- M2:** Same justification as for M2 under 84 cm. Substantial increased contribution to risk compared to 84 cm(A) scenario, due both to continued human-driven degradation of the ecosystems and the impacts of ocean warming and acidification. → Final score: [2] compared to 84 cm(A).
- M3:** Same justification as for M3 under 84 cm. Combination of very low-lying topographies with increased relative and extreme sea levels. → Final score: [3] compared to 84 cm(A).
- M4:** Same justification as for M4 under 84 cm. Beaches sediment budgets will already be substantially affected as SLR in the 84 cm scenario, and the situation will become worst under higher SLR. As a result, less sediments will be available at the coast compared to the 84 cm situation. → Final score: [2] compared to 84 cm(A).
- M5:** Same justification as for M5 under 84 cm. Intense cumulative effects of reduction in both volume and quality for groundwater lenses, surface waters and soils, compared to the 84 cm situation. → Final score: [2] compared to 84 cm(A).
- M6:** No major additional adaptation efforts compared to today. Same score as for Present Day.
- M7:** No major additional adaptation efforts compared to today. Same score as for Present Day.
- M8:** No major additional adaptation efforts compared to today. Same score as for Present Day.
- M9:** Not considered for urban atoll islands.
- 110(B)
- M1:** As for 110 cm(A).
- M2:** As for 110 cm(A).
- M3:** As for 110 cm(A).
- M4:** As for 110 cm(A).
- M5:** As for 110 cm(A).
- M6:** Same as for ME 84 cm(B): while the development of adequate coastal defence structures will still provide some benefits in terms of risk reduction (e.g., flooding limitation), protection structures will not necessarily prevent seawater infiltration due to the permeable nature of the island substratum. So even adequate coastal protection will probably not eliminate risk (Hinkel et al., 2018). As a result, and given the low elevation and porous nature of the islands, one can hypothesise that higher SLR scenarios would weaken the additional benefits of coastal protection structures, although huge uncertainty remains on such a hypothesis. → Final score: [0] compared to 84 cm(B).
- M7:** It is virtually certain that any climate change scenario resulting in a 110 cm rise in sea level will also generate significant changes in the ocean chemical parameters (temperature, pH). Accordingly, risks to ecosystems associated with such a scenario will be high to very high (Section 5.3.4). In the same line as in n 84 cm(B), this results in a reduced contribution of this metric to risk reduction under the RCP8.5 upper end of the *likely* range. → Final score: [-1] compared to 110 cm(A), that is, [1] compared to 84 cm(B).
- M8:** The rationale is basically the same as for 84 cm(B), except that land scarcity is exacerbated under a higher SLR scenario (i.e., higher potential loss of land). However, it was considered that the above-mentioned progressive shift in relocation

approaches from within the capital island to neighbouring or artificial islands (see 84 cm(B)) will remain relevant even under the RCP8.5 upper end of the *likely* range. → Final score: [-3] compared to 84 cm(B).

M9: Not considered for urban atoll islands.

SM4.3.8.3 Large Tropical Agricultural Deltas

See complementary information in Section 4.3.4.2.1 and Sheet 1 of the SM4.3 datafile.

The deltas considered in this analysis are the Ganges-Brahmaputra-Meghna Delta and the Mekong River Delta. Both deltas are large (first and second largest deltas by area globally), low-lying and dominated by agricultural production. The risk assessment to SLR considers the entire delta area (not only the coastal fringe), for the following reasons:

- i) SLR will contribute in some deltas (e.g., tidal deltas) in increased salinity intrusion inland, so the direct impacts will be not only on the coastal fringes;
- ii) Some of the adaptation measures are easier if a whole delta system is considered: for example, basin-scale water (sediment) management (with all the inherent difficulties of course), but also in terms of relocation;
- iii) Delta level planning (e.g., the Mekong) already incorporates various delta-wide development scenarios, a couple of which are 'do not protect too much' and thus convert to saline livelihoods (aquaculture and more salt tolerant crop varieties) and preserve a freshwater environment.

Other coastal river deltas with different characteristics will exhibit different risks to SLR related coastal hazards. Influencing factors are for example smaller ratio of coastal areas to full delta plain area (e.g., Limpopo delta, Mozambique), steeper slope (e.g., Red River delta, Vietnam), higher share of urbanisation (e.g., Nile delta, Egypt), megacity at the coast (e.g., Jakarta, Indonesia), lower population density (e.g., Orinoco delta, Venezuela), already strong protection (e.g., Rhine delta, Netherlands), and strong subsidence (e.g., Jakarta, Indonesia).

Present Day

M1: Population densities are high in both deltas compared to average coastal population densities with 1,280 per km² for the Ganges-Brahmaputra-Meghna (Ericson et al., 2006) and 433 per km² for the Mekong delta (GSO, 2016). Asset densities are moderate as both deltas are agriculture-dominated (Hossain et al., 2018; Kondolf et al., 2018). Agricultural production contributes to GDP strongly (Smajgl et al., 2015; Hossain et al., 2018), thus agricultural fields are important assets. → The overall contribution of population and asset density to risk is moderate to high in the Mekong delta and high in the Ganges-Brahmaputra-Meghna. The overall risk is high [4].

M2: In both deltas, mangroves are partially cut (Ghosh et al., 2018; Veettil et al., 2018). Wetlands at the coast but also further inland are degraded (Quan et al., 2018; Rahman et al., 2018), floodplains are in many instances cut off from the river due to flood protection for agricultural fields by poldering or dykes (Rogers and Overeem, 2017; Ngan et al., 2018; Warner et al., 2018). → On the delta scale, the contribution of degraded coastal ecosystems to risk driven by SLR related hazards is moderate to high [3].

M3: Currently in both deltas riverine flooding dominates (Auerbach et al., 2015; Rahman and Rahman, 2015; Ngan et al., 2018). High tides and cyclones however can lead to considerable and sometimes catastrophic coastal flooding especially in the Ganges-Brahmaputra-Meghna Delta (Auerbach et al., 2015) (Rahman and Rahman, 2015). Low flows in the river, dredging for sand and thus river bed deepening and subsidence leads to stronger intrusion of tidal flood water (Minderhoud et al., 2017; Shammi et al., 2017). In both deltas, subsidence is increasing the probability of flooding (Brown et al., 2018). The contribution of coastal flooding to risk is currently moderate in the Mekong and high in the Ganges-Brahmaputra-Meghna when the entire delta is considered. → Overall score is moderate to high [3].

M4: Coastal and river bank erosion is already a serious problem in parts of both deltas (Anthony et al., 2015; Brown and Nicholls, 2015; Li et al., 2017), while other parts are prograding (Wilson and Goodbred Jr, 2015; Zoccarato et al., 2018). → Coastal erosion is happening but in light of the overall delta area, it only contributes moderately to the current delta risk when the entire delta plain is considered [2].

M5: Salinisation is already happening in many aquifers, soils and surface water in the coastal parts of both deltas (Ayers et al., 2017; Minderhoud et al., 2017; Shammi et al., 2017). However, many communities also take advantage of the saline water for saline aquaculture (Smajgl et al., 2015; Rahman et al., 2018). Furthermore, salinity of water and soil resources did not yet reach a level, where it would contribute to risk significantly at the delta scale and it is still a coastal phenomenon (Smajgl et al., 2015; Ayers et al., 2017) although in some years salinity intrusion can reach far inland such as in 2015 in the Mekong Delta (UNDP, 2016). Salinity is a threat for domestic water supply but currently rather localised in the coastal zone (Ayers et al., 2017; Kondolf et al., 2018). → The contribution of salinisation to overall risk at the delta scale is currently moderate [2].

M6: Both deltas have a partial protection with hard engineered defences such as sluice gates to prevent flooding, polders and dykes in some coastal stretches (Smajgl et al., 2015; Rogers and Overeem, 2017; Warner et al., 2018). Coastal defences do not cover the entire coastline. → The contribution of hard engineered coastal defences to risk reduction is moderate today [2].

M7: Today, level of implementation of measures to protect/restore natural buffers is still limited. There are ongoing efforts in both deltas to restore mangroves, for example (Quan et al., 2018;

Rahman et al., 2018). → The overall scale of these measures is rather small compared to the coastline length and thus the risk reduction effect is undetectable to moderate [1].

M8: Today, the implementation of planned relocation aiming at reducing the exposure of people, assets and infrastructure remains sporadic in the Mekong and Ganges-Brahmaputra-Meghna deltas. Coastal areas of the Ganges-Brahmaputra-Meghna Delta are very dynamic and dynamic community responses are well known (e.g., relocations in the char-lands (Islam and Khan, 2018) but this is not a planned relocation. → Risk reduction by retreat measures is currently undetectable on the delta scale [0].

M9: Today, level of implementation of measures aiming at reducing subsidence is very low (Schmidt, 2015; Schmitt et al., 2017) although the first efforts to restrict groundwater extraction are underway. → Risk reduction by subsidence reduction is currently undetectable on the delta scale [0].

43(A)

M1: Both deltas experience outmigration today (Huy and Nonneman, 2016; Adams and Kay, 2019) and this might increase in the future. Asset density might increase with economic development (Szabo et al., 2015; Hoang et al., 2018). → Overall, population and asset densities might remain high in the future, therefore a similar contribution to risk under 43 cm(A) than today was assumed [4].

M2: Compared to Present Day and without enhanced adaptation action coastal ecosystems will be under increasing exposure to floods, erosion, cyclones, etc. (Li et al., 2017; Brown et al., 2018). Only when protected, sustainably managed and not squeezed, coastal ecosystems could keep up with SLR (Brown et al., 2018; Kondolf et al., 2018). → Without increased adaptation action and ecosystem management/protection, an increase of risk mainly caused by further degradation was assumed [1].

M3: Compared to Present Day, without increased adaptation action and no action to held subsidence, coastal flooding will contribute very substantially to increasing risk (Erban et al., 2014; Brown and Nicholls, 2015; Zoccarato et al., 2018). → The additional contribution to overall risk at the delta scale will be substantial [2].

M4: Compared to Present Day, without increased adaptation action and no action to hold subsidence, coastal erosion will increase due to SLR, subsidence, increased wave action and extreme events (Schmitt et al., 2017; Dang et al., 2018). → The additional contribution to overall risk at the delta scale remains moderate given that large share of the delta area will not be directly affected [1].

M5: If no action taken to increase adaptation and limit subsidence, salinisation of coastal waters and soils will be significant (Vu et al., 2018; Zoccarato et al., 2018; Rakib et al., 2019). →

Salinisation will contribute to risk substantially with impacts on agriculture, water supply etc. [2]

M6: No major additional adaptation efforts compared to today. Same score as for Present Day.

M7: No major additional adaptation efforts compared to today. Same score as for Present Day.

M8: No major additional adaptation efforts compared to today. Same score as for Present Day.

M9: No major additional adaptation efforts compared to today. Same score as for Present Day.

43(B)

M1: As for 43 cm(A).

M2: As for 43 cm(A).

M3: As for 43 cm(A).

M4: As for 43 cm(A).

M5: As for 43 cm(A).

M6: Additional contribution of enhanced adequately calibrated structures to decreasing risk, relative to business-as-usual interventions in the 43 cm(A) scenario. The implementation of hybrid defences is assumed with strong contribution of ecosystem-based adaptation combined with hard engineered coastal defences (Melillo, 2014; Hill, 2015). → Overall, the risk reduction contribution of hard engineered measures remains moderate in this scenario on the delta scale [−1].

M7: Additional contribution of ecosystem restoration efforts to decreasing risk (Dasgupta et al., 2019; Nguyen and Parnell, 2019), relative to business-as-usual interventions in the 43 cm(A) scenario in these agriculture dominated deltas (Schmitt et al., 2013; Van Cuong et al., 2015; Rahman et al., 2018). Despite this, human- and climate-driven disturbances on natural buffer ecosystems will not be fully removed as population and assets density will remain high in large tropical agricultural deltas (Davis et al., 2018; Uddin et al., 2019; Whitehead et al., 2019). → Overall, the risk reduction contribution of hard engineered measures remains moderate in this scenario on the delta scale [−2].

M8: It is assumed that hybrid protection effectively reduces the risk at 43 cm SLR (Al Masud et al., 2018; Van Coppenolle et al., 2018), thus relocation will not contribute substantially to the reduction of risk at the delta scale. → Same as Present Day.

M9: It is assumed that measures to lower subsidence will contribute to reduce the risk at 43 cm SLR. Since the reduction of subsidence would have impact on the risk level in large parts of the delta

(Nicholls et al., 2016; Schmitt et al., 2017), risk reduction effects will be felt on large scale. → Substantial risk reduction on the delta scale [-2].

84(A)

M1: As for 43 cm(A).

M2: Without increased adaptation coastal ecosystems will be under increasing exposure to floods, erosion, cyclones etc. (Erban et al., 2014; Takagi et al., 2016). They will be largely degraded and will contribute to the increasing risk strongly at the coast and moderately on the delta scale. → Final score: [1] compared to 43 cm(A).

M3: Without increased adaptation action and no action to held subsidence, coastal flooding will contribute very substantially to increasing risk (Khan et al., 2013; Takagi et al., 2016; Carvalho and Wang, 2019). → Final score: [3] compared to 43 cm(A).

M4: Without increased adaptation action and no action to held subsidence coastal erosion will increase due to SLR (Erban et al., 2014; Uddin et al., 2019), subsidence, increased wave action and extreme events. The additional contribution to overall risk at the delta scale will be substantially stronger than with 43 cm given that impacts will be felt more inland (Chen and Mueller, 2018; Vu et al., 2018). → Final score: [2] compared to 43 cm(A).

M5: Without increased no adaptation action and no action to held subsidence salinity intrusion will contribute substantially to risk as groundwater, soil and surface water will be salinised far inland. → Final score: [2] compared to 43 cm(A).

M6: No major additional adaptation efforts compared to today. Same score as for Present Day.

M7: No major additional adaptation efforts compared to today. Same score as for Present Day.

M8: No major additional adaptation efforts compared to today. Same score as for Present Day.

M9: No major additional adaptation efforts compared to today. Same score as for Present Day.

84(B)

M1: As for 84 cm(A).

M2: As for 84 cm(A).

M3: As for 84 cm(A).

M4: As for 84 cm(A).

M5: As for 84 cm(A).

M6: More engineered coastal defences will be implemented within the grey-green defence continuum (Yamamoto and Esteban, 2015). Risk reduction is substantial. → Final score: [-2] compared to 84 cm(A).

M7: At 84 cm SLR the role of coastal ecosystems in reducing risk will be limited (low additional contribution). → Final score: [-1] compared to 84 cm(A).

M8: At 84 cm SLR migration is assumed to take place and policies can help here greatly to reduce the risk (Chen and Mueller, 2018). Additional risk reduction potential is very substantial. → Final score: [-3] compared to 84cm(A).

M9: At 84 cm SLR the share of subsidence reduction in reducing the overall risk is smaller than at 43 cm SLR. → Final score: [-1] compared to 84 cm(A).

110(A)

M1: Same as for 84 cm(A)

M2: Without increased adaptation coastal ecosystems will be largely destroyed already at 84 cm (Schmitt et al., 2017; Mehvar et al., 2019; Mukul et al., 2019). No further increase in risk contribution is expected. → Final score: Same as at 84 cm(A).

M3: Without increased adaptation action, coastal flooding will contribute very substantially to increasing risk at the entire delta level (Huong and Pathirana, 2013; Brown et al., 2018; Dang et al., 2018). → Final score: [3] compared to 84 cm(A).

M4: Without increased adaptation action coastal erosion will increase due to SLR (Anthony et al., 2015; Liu et al., 2017; Uddin et al., 2019), increased wave action and extreme events. The additional contribution to overall risk at the delta scale will be substantial and stronger than with 84 cm given that impacts will be felt more inland. → Final score: [2] compared to 84 cm (A).

M5: With increased adaptation action salinity intrusion will contribute substantially to risk as groundwater, soil and surface water will be salinised far inland (Tran Anh et al., 2018; Rakib et al., 2019). It will strongly impact agriculture and water supply in the entire delta (Jiang et al., 2018; Timsina et al., 2018; Nhung et al., 2019). → Final score: [3] compared to 84 cm(A).

M6: No major additional adaptation efforts compared to today. Same score as for Present Day.

M7: No major additional adaptation efforts compared to today. Same score as for Present Day.

M8: No major additional adaptation efforts compared to today. Same score as for Present Day.

M9: No major additional adaptation efforts compared to today. Same score as for Present Day.

110(B)

M1: As for 110 cm(A).**M2:** As for 110 cm(A).**M3:** As for 110 cm(A).**M4:** As for 110 cm(A).**M5:** As for 110 cm(A).**M6:** Efforts towards the development of adequate coastal defence structures will provide substantial benefits in terms of risk reduction (Bhuiyan and Dutta, 2012; Danh and Khai, 2014). → Final score: [-3] compared to 110 cm(A).**M7:** At 110 cm SLR the role of ecosystems in risk reduction is reduced (Doughty et al., 2019; Mukul et al., 2019), they provide only a low to non-detectable contribution to risk reduction. → Final score: [0] compared to 110 cm(A).**M8:** Coastal relocation has a substantial potential to contribute risk reduction due to restricted habitability, livelihood options in the remaining delta area (Bhuiyan and Dutta, 2012). → Final score: [-3] compared to 110 cm(A).**M9:** At 110 cm, the share of subsidence reduction in reducing the overall risk is low (Payo et al., 2016; Zoccarato et al., 2018). → Final score: [-1] compared to 110 cm(A).

SM4.3.8.4 Arctic Communities (Remote From Regions of Rapid Glacio-Isostatic Adjustment)

See complementary information in Section 4.3.4.2.1 and Sheet 1 of the Excel SM4.3 datafile.

The communities considered in this analysis are small indigenous settlements located on the Arctic Coastal Plain. They lie on exposed coasts composed of un lithified ice-rich sediments in permafrost, all in areas of slow SLR, with seasonal sea ice and lengthening open-water seasons. More broadly in the Arctic, coastal communities with a variety of cultural, socio-economic and institutional characteristics, a wide range of population size from <150 (e.g., Sachs Harbour and Grise Fiord, Canada) to ~300,000 (Murmansk, Russian Federation), and a variety of coastal settings will exhibit different vulnerability (Forbes, 2011; Ford et al., 2016). In particular, communities located in areas of rapid GIA, such that relative sea level projections are negative (falling sea level) for all realistic emission scenarios and pathways this century (James, 2014; James et al., 2015; Forbes et al., 2018), have very low sensitivity to sea level change. In this analysis, however, only selected Arctic communities remote from regions of rapid GIA have been considered, more precisely:

- Bykovsky, Sakha Republic, Russian Federation (Lena Delta)
- Shishmaref, Alaska, USA
- Kivalina, Alaska, USA

- Shingle Point, Inuvialuit Settlement Region, Canada (Mackenzie Delta)
- Tuktoyaktuk, Inuvialuit Settlement Region, Canada (Mackenzie Delta)

Present Day

M1: Shishmaref and Kivalina are located on low-lying barrier islands formed by wave action and highly susceptible to variations in sea level (Marino, 2012; Bronen and Chapin, 2013; Fang et al., 2018; Rolph et al., 2018). Erosion has always been a problem, there is limited space to build, and there are few locations if any with low exposure. Shingle Point is similarly situated on an active gravel spit. Tuktoyaktuk is partly built on low ground with very high concentrations of massive ice, leading to rapid shoreline erosion, and extensive areas are flooded by storm surges at present sea level. Bykovsky is mostly situated at higher elevation, but erosion is nevertheless a problem. → In such sensitive and constraining environments, the overall contribution of population and asset density to risk is considered rather high, that is, a score of [4].**M2:** Accelerating permafrost thaw is promoting erosion of ice-rich sediments at Bykovsky and Tuktoyaktuk. In addition, sea ice and its decreasing extent, with a lengthening open-water season, provides less protection from storm impacts, particularly later in the year (Lantuit et al., 2011; Melvin et al., 2017). Furthermore, extensive critical ecosystems, especially the Lena and Mackenzie deltas, which provide food and other ecosystem services to nearby communities, are at risk today (Emmertson et al., 2007; Forbes, 2019). → Score [5].**M3:** High flooding risk today for Kivalina, Shishmaref, Shingle Point, Tuktoyaktuk and parts of the Mackenzie and Lena deltas (less so for Bykovsky). In Shishmaref, for example, 10 flooding events (1973–2015) resulted in emergency declarations (Solomon, 2005; Bronen and Chapin, 2013; Lamoureux et al., 2015; Albert et al., 2018; Fang et al., 2018; Irrgang et al., 2019). → Score [4].**M4:** Rapid erosion of ice-rich slopes below residences and other amenities at Bykovsky (Myers, 2005; Lantuit et al., 2011; Vanderlinden et al., 2018); likewise at Shishmaref and Kivalina (Bronen and Chapin, 2013; Albert et al., 2018; Fang et al., 2018), and at Tuktoyaktuk and vicinity (Lamoureux et al., 2015; Ford et al., 2016). → Score [5].**M5:** No evidence of salinisation issues in communities, but brackish water flooding of the outer Mackenzie Delta caused by a 1999 storm surge (a rare event due to upwelling ahead of the storm) led to widespread die off of vegetation with negative ecosystem impacts (Pisaric et al., 2011; Kokelj et al., 2012). → Score [2].**M6:** Some existing hard protection in Shishmaref and Tuktoyaktuk (Marino, 2012; Bronen and Chapin, 2013; Lamoureux et al., 2015; Ford et al., 2016). → Score [-1].

M7: No evidence of attention to natural buffers. Not possible for sea ice. → Score [0].

M8: Recognition of the need for possible relocation from eroding bluff in Bykovsky (Vanderlinden et al., 2018) and similarly in Tuktoyaktuk, where some facilities (e.g., police, school) have already been relocated (Lamoureux et al., 2015). A new suburb has been established in Tuktoyaktuk but is unpopular because of isolation and there is a strong desire to maintain the historical settlement footprint. In Shishmaref and Kivalina, relocation policies have been discussed but not implemented, with many challenges identified (Marino, 2012; Bronen and Chapin, 2013; Marino and Lazrus, 2015; Albert et al., 2018). → Score [-1].

M9: Not considered for Arctic communities.

43(A)

M1: Modest increase in exposed assets and reflection of population growth with few options to build new infrastructure (Hamilton et al., 2016).

M2: SLR effects exacerbated by increasing permafrost thaw and thermal degradation of ice-rich slopes with climate warming, and ongoing loss of sea ice. This results in increased risk to delta ecosystems (Vermaire et al., 2013; Lamoureux et al., 2015; Melvin et al., 2017; Vanderlinden et al., 2018; Forbes, 2019), and increased contribution of their degradation to risk reduction.

M3: Increased risk of coastal flooding in communities (except Bykovsky) and delta ecosystems. In Shishmaref, projected SLR and reduced ice cover are projected to increase flooding and erosion significantly (Melvin et al., 2017; Hoegh-Guldberg et al., 2018).

M4: As for M3, with erosion further accelerated by permafrost thaw (Lamoureux et al., 2015; Melvin et al., 2017).

M5: Possible risk of more extensive salinisation, for example, in the Mackenzie Delta.

M6: No major additional adaptation efforts compared to today. Same score as for Present Day.

M7: Little can be done. No way to restore lost ice.

M8: Under (A) scenario, the significant cost and social capital required for relocation would limit such policies, and therefore no further risk reduction compared to today.

M9: Not considered for Arctic communities.

43(B)

M1: As for 43 cm(A).

M2: As for 43 cm(A). Sea ice loss and permafrost thaw projected to continue.

M3: As for 43 cm(A).

M4: As for 43 cm(A), but with some potential for erosion to be reduced by adaptation.

M5: As for 43 cm(A).

M6: There are few opportunities even with current rates of change. Potential adaptations include shoreline protection or seawall construction, which may have some value in reducing flooding, but past experience is not encouraging and long-term effectiveness open to question (Sussman et al., 2014; Melvin et al., 2017; Fang et al., 2018). → Score [-1] compared to 43 cm(A).

M7: As for 43 cm(A).

M8: Limited governance stability or resources for action in Bykovsky (Vanderlinden et al., 2018), but overall, relocation could contribute to some risk reduction compared to scenario (A).

M9: Not considered for Arctic communities.

84(A)

M1: Same rationale as for 43 cm(A), with increase in exposed assets in some places and higher sea level making asset density more challenging.

M2: Exacerbation of permafrost thaw and thermal degradation of ice-rich slopes, increased risk to delta ecosystems including Lena Delta Wildlife Reserve and Kendall Island Bird Sanctuary and ongoing loss of sea ice.

M3: Increased risk of flooding, particularly in the outer deltas (Fedorova et al., 2015; Forbes, 2019), with much more extensive flooding in Kivalina and Shishmaref (Melvin et al., 2017).

M4: Accelerated erosion at all sites.

M5: Risk of more extensive salinisation in Mackenzie Delta and potential impacts on barrier island settlements.

M6: No risk reduction anticipated for scenario (A) given challenges outlined above.

M7: No change, little attention to natural buffers, and no way to address some such as lost sea ice.

M8: As for 43 cm(A).

M9: Not considered for Arctic communities.

*84(B)***M1:** As for 84 cm(A).**M2:** As for 84 cm(A).**M3:** As for 84 cm(A).**M4:** As for 84 cm(A).**M5:** As for 84 cm(A).**M6:** Even under scenario (B) there are probably few additional options, but demands for more shore protection will be louder in Tuktoyaktuk. The effectiveness of hard-engineered protection structures may however be limited by permafrost thaw.**M7:** As for 84 cm(A).**M8:** Possibly some local ad hoc action on relocation from eroding bluffs at Bykovsky, although lack of governance stability or effectiveness limits action (Vanderlinden et al., 2018); some additional relocation of assets will probably occur in Tuktoyaktuk and Shingle Point. SLR of this magnitude may provide additional impetus for community relocation in Shishmaref and Kivalina. Therefore, there is substantial effect on risk reduction compared to 43 cm(B).**M9:** Not considered for Arctic communities.*110(A)***M1:** Probable increase in exposed assets.**M2:** Increased risk to delta ecosystems as well as ongoing deeper thaw and loss of sea ice. Possible natural aggradation of barrier islands and spits at Shishmaref, Kivalina, and Shingle Point (Irrgang et al., 2018), but would be accompanied by flooding and infrastructure damage.**M3:** Increased risk of flooding (deltas and communities).**M4:** Accelerated erosion at all sites.**M5:** Enhanced risk in Mackenzie Delta.**M6:** As for 84(A).**M7:** As for 84(A).**M8:** As for 84(A).**M9:** Not considered for Arctic communities.*110(B)***M1:** As for 110 cm(A).**M2:** As for 110 cm(A).**M3:** As for 110 cm(A).**M4:** As for 110 cm(A).**M5:** As for 110 cm(A).**M6:** Enhanced shore protection at Tuktoyaktuk, but in Shishmaref and Kivalina there are probably few additional options for adaptation. As for 84 cm(B), the effectiveness of hard-engineered protection structures may however be limited by permafrost thaw.**M7:** As for 84 cm(B).**M8:** As for 84 cm(B). While some further community-led relocation in Shishmaref and Kivalina, for example, offers a way to reduce risk, it also faces many barriers.**M9:** Not considered for Arctic communities.

References

- Adams, H. and S. Kay, 2019: Migration as a human affair: Integrating individual stress thresholds into quantitative models of climate migration. *Environ. Sci. Pol.*, **93**, 129–138.
- Aitken, A.R.A. et al., 2016: Repeated large-scale retreat and advance of Totten Glacier indicated by inland bed erosion. *Nature*, **533**, 385, doi:10.1038/nature17447.
- Al Masud, M.M., N.N. Moni, H. Azadi and S. Van Passel, 2018: Sustainability impacts of tidal river management: Towards a conceptual framework. *Ecol. Indic.*, **85**, 451–467.
- Albert, S. et al., 2018: Heading for the hills: climate-driven community relocations in the Solomon Islands and Alaska provide insight for a 1.5°C future. *Reg. Environ. Change*, **18**(8), 2261–2272.
- Anthony, E.J. et al., 2015: Linking rapid erosion of the Mekong River delta to human activities. *Sci. Rep.*, **5**, 14745, doi:10.1038/srep14745.
- Auerbach, L. et al., 2015: Flood risk of natural and embanked landscapes on the Ganges–Brahmaputra tidal delta plain. *Nat. Clim. Change*, **5**(2), 153.
- Austermann, J., J.X. Mitrovica, P. Huybers and A. Rovere, 2017: Detection of a dynamic topography signal in last interglacial sea-level records. *Sci. Adv.*, **3**(7), e1700457.
- Austermann, J. et al., 2015: The impact of dynamic topography change on Antarctic ice sheet stability during the mid-Pliocene warm period. *Geology*, **43**(10), 927–930, doi:10.1130/g36988.1.
- Ayers, J. C. et al., 2017: Salinization and arsenic contamination of surface water in southwest Bangladesh. *Geochemical Geochem. Trans.*, **18**(1), 4.
- Badger, M.P., D.N. Schmidt, A. Mackensen and R.D. Pancost, 2013: High-resolution alkenone palaeobarometry indicates relatively stable pCO₂ during the Pliocene (3.3–2.8 Ma). *Philos. Trans. R. Soc. A.*, **371**(2001), 20130094, doi:10.1098/rsta.2013.0094.
- Bailey, R.T., K. Barnes and C.D. Wallace, 2016: Predicting Future Groundwater Resources of Coral Atoll Islands. *Hydrol. Process.*, **30**(13), 2092–2105.
- Bailey, R.T., A. Khalil and V. Chatikavanij, 2014: Estimating transient freshwater lens dynamics for atoll islands of the Maldives. *J. Hydrol.*, **515**, 247–56.
- Bamber, J.L., R.E. Riva, B.L.A. Vermeersen and A.M. LeBrocq, 2009: Reassessment of the potential sea-level rise from a collapse of the West Antarctic Ice Sheet. *Science*, **324**(5929), 901–903, doi:10.1126/science.1169335.
- Barlow, N.L.M. et al., 2018: Lack of evidence for a substantial sea-level fluctuation within the Last Interglacial. *Nat. Geosci.*, **11**(9), 627–634, doi:10.1038/s41561-018-0195-4.
- Beetham, E., P.S. Kench and S. Popinet, 2017: Future Reef Growth Can Mitigate Physical Impacts of Sea-Level Rise on Atoll Islands. *Earth's Future*, **5**(10), 1002–1014.
- Bertram, R.A. et al., 2018: Pliocene deglacial event timelines and the biogeochemical response offshore Wilkes Subglacial Basin, East Antarctica. *Earth Planet. Sci. Lett.*, **494**, 109–116, doi:10.1016/j.epsl.2018.04.054.
- Bhuiyan, M.J.A.N. and D. Dutta, 2012: Assessing impacts of sea level rise on river salinity in the Gorai river network, Bangladesh. *Estuar. Coast. Shelf Sci.*, **96**, 219–227.
- Bierman, P.R. et al., 2016: A persistent and dynamic East Greenland Ice Sheet over the past 7.5 million years. *Nature*, **540**(7632), 256.
- Biribo, N. and C.D. Woodroffe, 2013: Historical area and shoreline change of reef islands around Tarawa Atoll, Kiribati. *Sustain. Sci.*, **8**(3), 345–362.
- Blanchon, P., A. Eisenhauer, J. Fietzke and V. Liebetau, 2009: Rapid sea-level rise and reef back-stepping at the close of the last interglacial highstand. *Nature*, **458**, 881–884.
- Bronen, R. and F.S. Chapin, 2013: Adaptive governance and institutional strategies for climate-induced community relocations in Alaska. *PNAS*, **110**(23), 9320–9325.
- Brown, S. and R. Nicholls, 2015: Subsidence and human influences in mega deltas: the case of the Ganges–Brahmaputra–Meghna. *Sci. Total Environ.*, **527**, 362–374.
- Brown, S. et al., 2018: What are the implications of sea-level rise for a 1.5, 2 and 3°C rise in global mean temperatures in the Ganges–Brahmaputra–Meghna and other vulnerable deltas? *Reg. Environ. Change*, **18**(6), 1829–1842.
- Burke, K.D. et al., 2018: Pliocene and Eocene provide best analogs for near-future climates. *PNAS*, **115**(52), 13288–13293, doi:10.1073/pnas.1809600115.
- Capron, E. et al., 2014: Temporal and spatial structure of multi-millennial temperature changes at high latitudes during the Last Interglacial. *Quat. Sci. Rev.*, **103**, 116–133.
- Carvalho, K. and S. Wang, 2019: Characterizing the Indian Ocean sea level changes and potential coastal flooding impacts under global warming. *J. Hydrol.*, **569**, 373–386.
- Chen, J. and V. Mueller, 2018: Coastal climate change, soil salinity and human migration in Bangladesh. *Nat. Clim. Change*, **8**(11), 981.
- Colleoni, F. et al., 2018: Past continental shelf evolution increased Antarctic ice sheet sensitivity to climatic conditions. *Sci. Rep.*, **8**(1), 11323, doi:10.1038/s41598-018-29718-7.
- Colleoni, F. et al., 2014: Modeling Northern Hemisphere ice-sheet distribution during MIS 5 and MIS 7 glacial inception. *Clim. Past*, **10**(1), 269–291, doi:10.5194/cp-10-269-2014.
- Cook, C.P. et al., 2013: Dynamic behaviour of the East Antarctic ice sheet during Pliocene warmth. *Nat. Geosci.*, **6**(9), 765–769, doi:10.1038/ngeo1889.
- Dahl-Jensen, D. et al., 2013: Eemian interglacial reconstructed from a Greenland folded ice core. *Nature*, **493**(7433), 489–494, doi:10.1038/nature11789.
- Dang, T.D., T.A. Cochrane and M.E. Arias, 2018: Future hydrological alterations in the Mekong Delta under the impact of water resources development, land subsidence and sea level rise. *J. Hydrol.: Regional Studies*, **15**, 119–133.
- Danh, V. and H. Khai, 2014: Using a risk cost-benefit analysis for a sea dike to adapt to the sea level in the Vietnamese Mekong River Delta. *Climate*, **2**(2), 78–102.
- Dasgupta, S. et al., 2019: Quantifying the protective capacity of mangroves from storm surges in coastal Bangladesh. *PLoS one*, **14**(3), e0214079.
- Davis, K.F., A. Bhattachan, P. D'Odorico and S. Suweis, 2018: A universal model for predicting human migration under climate change: examining future sea level rise in Bangladesh. *Environ. Res. Lett.*, **13**(6), 064030.
- de Boer, B. et al., 2015: Simulating the Antarctic ice sheet in the late-Pliocene warm period: PLISMIP-ANT, an ice-sheet model intercomparison project. *The Cryosphere*, **9**, 881–903, doi:10.5194/tc-9-881-2015.
- de Boer, B. et al., 2017a: The Transient Response of Ice Volume to Orbital Forcing During the Warm Late Pliocene. *Geophys. Res. Lett.*, n/a-n/a, doi:10.1002/2017GL073535.
- de Boer, B., P. Stocchi, P.L. Whitehouse and R.S.J.Q.S.R. van de Wal, 2017b: Current state and future perspectives on coupled ice-sheet–sea-level modelling. **169**, 13–28.
- DeConto, R.M. and D. Pollard, 2016: Contribution of Antarctica to past and future sea-level rise. *Nature*, **531**(7596), 591–597, doi:10.1038/nature17145.
- Delta Programme, 2015: *Working on the Delta – The Decisions to Keep the Netherlands Safe and Liveable (Ministerie van Infrastructuur en Milieu)*. [Available at: <https://english.deltacommissaris.nl/documents/publications/2014/09/16/delta-programme-2015>].
- Dendy, S., J. Austermann, J. Creveling and J.J.Q.S.R. Mitrovica, 2017: Sensitivity of Last Interglacial sea-level high stands to ice sheet configuration during Marine Isotope Stage 6. **171**, 234–244.

- Dolan, A.M. et al., 2018: High climate model dependency of Pliocene Antarctic ice-sheet predictions. *Nat. Commun.*, **9**(1), 2799, doi:10.1038/s41467-018-05179-4.
- Donner, S.D. and S. Webber, 2014: Obstacles to climate change adaptation decisions: a case study of sea-level rise and coastal protection measures in Kiribati. *Sustain. Sci.*, **9**(3), 331–345.
- Doughty, C.L., K.C. Cavanaugh, R.F. Ambrose and E.D. Stein, 2019: Evaluating regional resiliency of coastal wetlands to sea level rise through hypsometry-based modeling. *Global Change Biol.*, **25**(1), 78–92.
- Düsterhus, A., M.E. Tamisiea and S. Jevrejeva, 2016: Estimating the sea level highstand during the last interglacial: a probabilistic massive ensemble approach. *Geophys. J. Int.*, **206**(2), 900–920, doi:10.1093/gji/ggw174.
- Dutton, A. et al., 2015a: Sea-level rise due to polar ice-sheet mass loss during past warm periods. *Science*, **349**(6244).
- Dutton, A., J.M. Webster, D. Zwartz and K. Lambeck, 2015b: Tropical tales of polar ice: evidence of Last Interglacial polar ice sheet retreat recorded by fossil reefs of the granitic Seychelles islands. *Quat. Sci. Rev.*, **107**, 182–196.
- Duvat, V., 2013: Coastal protection structures in Tarawa atoll, Republic of Kiribati. *Sustain. Sci.*, **8**(3), 363–379.
- Duvat, V., A. Magnan and F. Pouget, 2013: Exposure of atoll population to coastal erosion and flooding: a South Tarawa assessment, Kiribati. *Sustain. Sci.*, **8**(3), 423–440.
- Duvat, V.K., 2019: A global assessment of atoll island planform changes over the past decades. *WiRes. Clim. Change*, **10**–(1), e557.
- Edwards, T.L. et al., 2019: Revisiting Antarctic ice loss due to marine ice-cliff instability. *Nature*, **566**(7742), 58–64, doi:10.1038/s41586-019-0901-4.
- Elliff, C.I. and I.R. Silva, 2017: Coral reefs as the first line of defense: Shoreline protection in face of climate change. *Mar. Environ. Res.*, **127**, 148–154.
- Emmertson, C.A., L.F. Lesack and P. Marsh, 2007: Lake abundance, potential water storage, and habitat distribution in the Mackenzie River Delta, western Canadian Arctic. *Water Resour. Res.*, **43**(5), 1–14.
- Erban, L.E., S.M. Gorelick and H.A. Zebker, 2014: Groundwater extraction, land subsidence, and sea-level rise in the Mekong Delta, Vietnam. *Environ. Res. Lett.*, **9**(8), 084010.
- Ericson, J.P. et al., 2006: Effective sea-level rise and deltas: causes of change and human dimension implications. *Global Planet. Change*, **50**(1–2), 63–82.
- Fang, Z., P.T. Freeman, C.B. Field and K.J. Mach, 2018: Reduced sea ice protection period increases storm exposure in Kivalina, Alaska. *Arctic Science*, **4**(4), 525–537.
- Fedorova, I. et al., 2015: Lena Delta hydrology and geochemistry: long-term hydrological data and recent field observations. *Biogeosciences*, **12**(2), 345–363.
- Fischer, H. et al., 2018: *Palaeoclimate constraints on the impact of 2°C anthropogenic warming and beyond*. 474–485 pp.
- Fogwill, C.J. et al., 2014: Testing the sensitivity of the East Antarctic Ice Sheet to Southern Ocean dynamics: past changes and future implications. *J. Quat. Sci.*, **29**(1), 91–98, doi:10.1002/jqs.2683.
- Forbes, D.L., 2011: *State of the Arctic coast 2010: scientific review and outlook*. International Arctic Science Committee, Land-Ocean Interactions in the Coastal Zone, Arctic Monitoring and Assessment Programme, International Permafrost Association. Helmholtz-Zentrum, Geesthacht, Germany, 178 p. <http://arcticcoasts.org>.
- Forbes, D.L., 2019: Arctic Deltas and Estuaries: A Canadian Perspective. *Coasts and Estuaries*, Amsterdam-Oxford-Cambridge, ISBN: 978–0–12–814003–1, 701 p., 123–147.
- Forbes, D.L. et al., 2018: Coastal environments and drivers. In: *From Science to Policy in the Eastern Canadian Arctic: An Integrated Regional Impact Study (IRIS) of Climate Change and Moderization* [Bell, T. and T.M. Brown (eds.)]. ArcticNet, Quebec, 210–249.
- Ford, J., T. Bell and N. Couture, 2016: Perspectives of Canada's North Coast region. In: *Canada's Marine Coasts in a Changing Climate* [Lemmen, D.S., Warren, F.J., James, T.S., Mercer Clarke, C.S.L. (eds.)], Government of Canada, Ottawa, 280 p., 153–206.
- Fretwell, P. et al., 2013: Bedmap2: improved ice bed, surface and thickness datasets for Antarctica. *The Cryosphere*, **7**(1).
- Gasson, E., R.M. DeConto and D. Pollard, 2016: Modeling the oxygen isotope composition of the Antarctic ice sheet and its significance to Pliocene sea level. *Geology*, **44**(10), 827–830.
- Ghosh, M.K., L. Kumar and P.K. Langat, 2018: Mapping tidal channel dynamics in the Sundarbans, Bangladesh, between 1974 and 2017, and implications for the sustainability of the Sundarbans mangrove forest. *Environ. Monit. Assess.*, **190**(10), 582.
- Goelzer, H., P. Huybrechts, M.-F. Loutre and T. Fichet, 2016: Last Interglacial climate and sea-level evolution from a coupled ice sheet–climate model. *Clim. Past*, **12**, 2195–2213, doi:10.5194/cp-12-2195-2016.
- Golledge, N.R., R.H. Levy, R.M. McKay and T.R. Naish, 2017: East Antarctic ice sheet most vulnerable to Weddell Sea warming. *Geophys. Res. Lett.*, **44**(5), 2343–2351, doi:10.1002/2016GL072422.
- GSO, 2016: *Statistical Yearbook of Vietnam*. Hanoi. URL: www.gso.gov.vn/default_en.aspx?tabid=515&idmid=5&ItemID=18533.
- Hamilton, L.C. et al., 2016: Climigration? Population and climate change in Arctic Alaska. *Popul. Environ.*, **38**(2), 115–133.
- Haywood, A.M., H.J. Dowsett and A.M. Dolan, 2016: Integrating geological archives and climate models for the mid-Pliocene warm period. *Nat. Commun.*, **7**, doi:10.1038/ncomms10646.
- Helsen, M.M. et al., 2013: Coupled regional climate–ice-sheet simulation shows limited Greenland ice loss during the Eemian. *Clim. Past*, **9**(4), 1773–1788, doi:10.5194/cp-9-1773-2013.
- Hill, K., 2015: Coastal infrastructure: a typology for the next century of adaptation to sea-level rise. *Front. Ecol. Environ.*, **13**(9), 468–476.
- Hinkel, J. et al., 2018: The ability of societies to adapt to twenty-first-century sea-level rise. *Nat. Clim. Change*, **8**(7), 570–578, doi:10.1038/s41558-018-0176-z.
- Hoang, L.P. et al., 2018: Managing flood risks in the Mekong Delta: How to address emerging challenges under climate change and socioeconomic developments. *Ambio*, **47**(6), 635–649.
- Hoegh-Guldberg, O. et al., 2018: Impacts of 1.5 °C global warming on natural and human systems In: *Global Warming of 1.5°C. An IPCC Special Report on the impacts of global warming of 1.5°C above pre-industrial levels and related global greenhouse gas emission pathways, in the context of strengthening the global response to the threat of climate change, sustainable development, and efforts to eradicate poverty*. [Masson-Delmotte, V., P. Zhai, H.-O. Pörtner, D. Roberts, J. Skea, P.R. Shukla, A. Pirani, W. Moufouma-Okia, C. Péan, R. Pidcock, S. Connors, J.B.R. Matthews, Y. Chen, X. Zhou, M.I. Gomis, E. Lonnoy, T. Maycock, M. Tignor and T. Waterfield (eds.)]. Cambridge University Press, Cambridge, United Kingdom and New York, NY, USA, 138 p.
- Hoeke, R.K. et al., 2013: Widespread inundation of Pacific islands triggered by distant-source wind-waves. *Global Planet. Change*, **108**, 128–138.
- Hoffman, J.S., P.U. Clark, A.C. Parnell and F. He, 2017: Regional and global sea-surface temperatures during the last interglaciation. *Science*, **355**(6322), 276–279.
- Hossain, M.A., M. Ahmed, E. Ojea and J.A. Fernandes, 2018: Impacts and responses to environmental change in coastal livelihoods of south-west Bangladesh. *Sci. Total Environ.*, **637**, 954–970.
- Hu, J.-J. et al., 2015: A new positive relationship between p CO₂ and stomatal frequency in *Quercus guyavifolia* (Fagaceae): a potential proxy for palaeo-CO₂ levels. *Ann. Bot.*, **115**(5), 777–788.
- Hughes, T.P. et al., 2017: Coral reefs in the Anthropocene. *Nature*, **546**(7656), 82.
- Huong, H.T.L. and A. Pathirana, 2013: Urbanization and climate change impacts on future urban flooding in Can Tho city, Vietnam. *Hydrol. Earth Syst. Sci.*, **17**(1), 379–394.
- Huy, H. T. and W. Nonneman, 2016: Economic effects of labor migration on agricultural production of farm households in the Mekong River Delta region of Vietnam. *Asian and Pacific Migration Journal*, **25**(1), 3–21.

- Irrgang, A.M. et al., 2019: Impacts of past and future coastal changes on the Yukon coast – threats for cultural sites, infrastructure, and travel routes. *Arctic Science*, **5**(2), 107–126.
- Irrgang, A.M. et al., 2018: Variability in rates of coastal change along the Yukon coast, 1951 to 2015. *J. Geophys. Res.-Earth*, **123**(4), 779–800.
- Islam, M.R. and N.A. Khan, 2018: Threats, vulnerability, resilience and displacement among the climate change and natural disaster-affected people in South-East Asia: an overview. *Journal of the Asia Pacific Economy*, **23**, 1–27.
- James, T. S. et al., 2014: Relative sea-level projections in Canada and the adjacent mainland United States. *Geological Survey of Canada, Open File 7737*, 10.4095 10.4095. URL: http://publications.gc.ca/collections/collection_2016/rncan-nrcan/M183-2-7737-eng.pdf.
- James, T. et al., 2015: Tabulated values of relative sea-level projections in Canada and the adjacent mainland United States. *Geological Survey of Canada, Open File 7942*, 10.4095. URL: <https://geoscan.nrcan.gc.ca/starweb/geoscan/servlet.starweb?path=geoscan/fulle.web&search1=R=297048>.
- Jiang, Z. et al., 2018: Future changes in rice yields over the Mekong River Delta due to climate change – Alarming or alerting? *Theor. Appl. Climatol.*, **137**(1–2), 545–555.
- Khan, D.M. et al., 2013: Back to the future: assessing the impact of the 2004 flood in Dhaka in 2050. In: *Proceedings of the International Conference on Flood Resilience, Experiences in Asia and Europe*, 5–7.
- Koenig, S.J., R.M. DeConto and D. Pollard, 2014: Impact of reduced Arctic sea ice on Greenland ice sheet variability in warmer than present climate. *Geophys. Res. Lett.*, **41**(11), 3933–3942, doi:10.1002/2014GL059770.
- Kokelj, S.V. et al., 2012: Using multiple sources of knowledge to investigate northern environmental change: regional ecological impacts of a storm surge in the outer Mackenzie Delta, NWT. *Arctic*, 257–272.
- Kondolf, G.M. et al., 2018: Changing sediment budget of the Mekong: Cumulative threats and management strategies for a large river basin. *Sci. Total Environ.*, **625**, 114–134.
- Kopp, R.E. et al., 2017: Evolving Understanding of Antarctic Ice-Sheet Physics and Ambiguity in Probabilistic Sea-Level Projections. *Earth's Future*, **5**(12), 1217–1233, doi:10.1002/2017ef000663.
- Kopp, R.E. et al., 2009: Probabilistic assessment of sea level during the last interglacial stage. *Nature*, **462**(7275), 863–867, doi:10.1038/nature08686.
- Lambeck, K., A. Purcell and A. Dutton, 2012: The anatomy of interglacial sea levels: The relationship between sea levels and ice volumes during the Last Interglacial. *Earth Planet. Sci. Lett.*, **315–316**, 4–11, doi:10.1016/j.epsl.2011.08.026.
- Lamoureux, S. et al., 2015: The impact of climate change on infrastructure in the western and central Canadian Arctic. In: *From Science to Policy in the Western and Central Canadian Arctic: an Integrated Regional Impact Study (IRIS) of Climate Change and Modernization* [Stern, G.A. and A. Gaden (eds.)]. ArcticNet, Quebec, pp. 300–341.
- Landais, A. et al., 2016: How warm was Greenland during the last interglacial period? *Clim. Past*, **12**(9), 1933–1948, doi:10.5194/cp-12-1933-2016.
- Lantuit, H. et al., 2011: Coastal erosion dynamics on the permafrost-dominated Bykovsky Peninsula, north Siberia, 1951–2006. *Polar Res.*, **30**(1), 7341.
- Li, X., J.P. Liu, Y. Saito and V.L. Nguyen, 2017: Recent evolution of the Mekong Delta and the impacts of dams. *Earth-Sci. Rev.*, **175**, 1–17.
- Lisiecki, L.E. and M.E. Raymo, 2005: A Pliocene-Pleistocene stack of 57 globally distributed benthic 180 records. *Paleoceanography*, **20**(1).
- Liu, J.P. et al., 2017: Stratigraphic formation of the Mekong River Delta and its recent shoreline changes. *Oceanography*, **30**(3), 72–83.
- Marino, E., 2012: The long history of environmental migration: Assessing vulnerability construction and obstacles to successful relocation in Shishmaref, Alaska. *Global Environ. Change*, **22**(2), 374–381.
- Marino, E. and H. Lazrus, 2015: Migration or forced displacement?: the complex choices of climate change and disaster migrants in Shishmaref, Alaska and Nanumea, Tuvalu. *Hum. Organ.*, **74**(4), 341–350.
- Martínez-Botí, M.A. et al., 2015: Plio-Pleistocene climate sensitivity evaluated using high-resolution CO₂ records. *Nature*, **518**(7537), 49.
- Masson-Delmotte, V. et al., 2013: Information from Paleoclimate Archives. In: *Climate Change 2013: The Physical Science Basis: Contribution of Working Group I to the Fifth Assessment Report of the Intergovernmental Panel on Climate Change*. [Stocker, T.F., D. Qin, G.K. Plattner, M. Tignor, S.K. Allen, J. Boschung, A. Nauels, Y. Xia, V. Bex and P.M. Midgley (eds.)]. Cambridge University Press, Cambridge, United Kingdom and New York, NY, USA.
- McCubbin, S., B. Smit and T. Pearce, 2015: Where does climate fit? Vulnerability to climate change in the context of multiple stressors in Funafuti, Tuvalu. *Global Environ. Change*, **30**, 43–55.
- McFarlin, J.M. et al., 2018: Pronounced summer warming in northwest Greenland during the Holocene and Last Interglacial. *PNAS*, **115**(25), 6357–6362, doi:10.1073/pnas.1720420115.
- McIver, L. et al., 2015: Climate change, overcrowding and non-communicable diseases: The 'triple whammy' of tuberculosis transmission risk in Pacific atoll countries. *Annals of the ACTM: An International Journal of Tropical and Travel Medicine*, **16**(3), 57.
- McKay, N.P., J. Overpeck and B. Otto-Bliesner, 2011: The role of ocean thermal expansion in Last Interglacial sea level rise. *Geophys. Res. Lett.*, **38**, L14605, doi:10.1029/2011GL048280.
- McLean, R. and P. Kench, 2015: Destruction or persistence of coral atoll islands in the face of 20th and 21st century sea-level rise? *WiRes. Clim. Change*, **6**(5), 445–463.
- Mehvar, S. et al., 2019: Climate change-driven losses in ecosystem services of coastal wetlands: A case study in the West coast of Bangladesh. *Ocean Coast. Manage.*, **169**, 273–283.
- Melillo, J.M., 2014: *Climate change impacts in the United States: the third national climate assessment*. Government Printing Office, Washington, 841 p. ISBN: SBN 9780160924026.
- Melvin, A.M. et al., 2017: Climate change damages to Alaska public infrastructure and the economics of proactive adaptation. *PNAS*, **114**(2), E122–E131.
- Miller, K.G. et al., 2012: High tide of the warm Pliocene: Implications of global sea level for Antarctic deglaciation. *Geology*, doi:10.1130/g32869.1.
- Minderhoud, P. et al., 2017: Impacts of 25 years of groundwater extraction on subsidence in the Mekong delta, Vietnam. *Environ. Res. Lett.*, **12**(6), 064006.
- Morlighem, M. et al., 2017: BedMachine v3: Complete bed topography and ocean bathymetry mapping of Greenland from multibeam echo sounding combined with mass conservation. *Geophys. Res. Lett.*, **44**(21), 11051–11061, doi:10.1002/2017GL074954.
- Mukul, S.A. et al., 2019: Combined effects of climate change and sea-level rise project dramatic habitat loss of the globally endangered Bengal tiger in the Bangladesh Sundarbans. *Sci. Total Environ.*, **663**, 830–840.
- Myers, S.L., Revkin, A.C., Romero, S., Krauss, C., 2005: Old ways of life are fading as the Arctic thaws. *The New York Times*, Oct. 20, 2005.
- Naish, T. et al., 2009: Obliquity-paced, Pliocene West Antarctic Ice Sheet oscillations. *Nature*, **458**, 322–328, doi:10.1038/nature07867.
- Naish, T. and G.S. Wilson, 2009: Constraints on the amplitude of Mid-Pliocene (3.6–2.4 Ma) eustatic sea-level fluctuations from the New Zealand shallow-marine sediment record. *Philos. Trans. Roy. Soc. A*, **367**, 169–187, doi:10.1098/rsta.2008.0223.
- Naylor, A.K., 2015: Island morphology, reef resources, and development paths in the Maldives. *Progr. Phys. Geogr.*, **39**(6), 728–749.
- Ngan, L.T. et al., 2018: Interplay between land-use dynamics and changes in hydrological regime in the Vietnamese Mekong Delta. *Land use policy*, **73**, 269–280.
- Nguyen, T.P. and K.E. Parnell, 2019: Coastal land use planning in Ben Tre, Vietnam: constraints and recommendations. *Heliyon*, **5**(4), e01487.
- Nhung, T.T., P. Le Vo, V. Van Nghi and H.Q. Bang, 2019: Salt intrusion adaptation measures for sustainable agricultural development under climate change effects: A case of Ca Mau Peninsula, Vietnam. *Clim. Risk Manage.*, **23**, 88–100.

- Nicholls, R. et al., 2016: Integrated assessment of social and environmental sustainability dynamics in the Ganges-Brahmaputra-Meghna delta, Bangladesh. *Estuar. Coast. Shelf Sci.*, **183**, 370–381.
- Oberle, F., P. Swarzenski and C. Storlazzi, 2017: Atoll groundwater movement and its response to climatic and sea-level fluctuations. *Water*, **9**(9), 650.
- Onaka, S. et al., 2017: Effectiveness of gravel beach nourishment on Pacific Island. In: *Asian And Pacific Coast 2017: Proceedings Of The 9th International Conference On Apac 2017* [Suh, K.-D., E.C. Cruz and Y. Tajima (eds.)]. World Scientific, Singapore, 952 p., ISBN 978-981-3233-80-9.
- Patterson, M.O. et al., 2014: Orbital forcing of the East Antarctic ice sheet during the Pliocene and Early Pleistocene. *Nat. Geosci.*, **7**, 841–847, doi:10.1038/ngeo2273.
- Payo, A. et al., 2016: Projected changes in area of the Sundarban mangrove forest in Bangladesh due to SLR by 2100. *Clim. Change*, **139**(2), 279–291.
- Pendleton, L. et al., 2016: Coral reefs and people in a high-CO2 world: Where can science make a difference to people? *PLoS one*, **11**(11), e0164699.
- Perry, C. and K. Morgan, 2017: Post-bleaching coral community change on southern Maldivian reefs: is there potential for rapid recovery? *Coral Reefs*, **36**(4), 1189–1194.
- Perry, C.T. et al., 2018: Loss of coral reef growth capacity to track future increases in sea level. *Nature*, **558**(7710), 396.
- Pisaric, M.F. et al., 2011: Impacts of a recent storm surge on an Arctic delta ecosystem examined in the context of the last millennium. *PNAS*, **108**(22), 8960–8965.
- Plach, A. et al., 2018: Eemian Greenland SMB strongly sensitive to model choice. *Clim. Past*, **14**(10), 1463–1485, doi:10.5194/cp-14-1463-2018.
- Pollard, D., R.M. DeConto and R.B. Alley, 2015: Potential Antarctic Ice Sheet retreat driven by hydrofracturing and ice cliff failure. *Earth Planet. Sci. Lett.*, **412**, 112–121.
- Post, V.E. et al., 2018: On the resilience of small-island freshwater lenses: Evidence of the long-term impacts of groundwater abstraction on Bonriki Island, Kiribati. *J. Hydrol.*, **564**, 133–148.
- Quan, N.H. et al., 2018: Conservation of the Mekong Delta wetlands through hydrological management. *Ecol. Res.*, **33**(1), 87–103.
- Quataert, E. et al., 2015: The influence of coral reefs and climate change on wave-driven flooding of tropical coastlines. *Geophys. Res. Lett.*, **42**(15), 6407–6415.
- Quiquet, A., C. Ritz, H.J. Punge and D. Salas y Mélia, 2013: Greenland ice sheet contribution to sea level rise during the last interglacial period: a modelling study driven and constrained by ice core data. *Clim. Past*, **9**(1), 353–366, doi:10.5194/cp-9-353-2013.
- Rahman, M.A. and S. Rahman, 2015: Natural and traditional defense mechanisms to reduce climate risks in coastal zones of Bangladesh. *Weather and Climate Extremes*, **7**, 84–95.
- Rahman, M.M., Y. Jiang and K. Irvine, 2018: Assessing wetland services for improved development decision-making: a case study of mangroves in coastal Bangladesh. *Wetl. Ecol. Manag.*, **26**(4), 563–580.
- Rakib, M., J. Sasaki, H. Matsuda and M. Fukunaga, 2019: Severe salinity contamination in drinking water and associated human health hazards increase migration risk in the southwestern coastal part of Bangladesh. *J. Environ. Manage.*, **240**, 238–248.
- Raymo, M.E. et al., 2018: The accuracy of mid-Pliocene $\delta^{18}O$ -based ice volume and sea level reconstructions. *Earth-Sci. Rev.*, **177**, 291–302, doi:10.1016/j.earscirev.2017.11.022.
- Raymo, M.E., L.E. Lisiecki and K.H. Nisancioglu, 2006: Plio-Pleistocene ice volume, Antarctic climate, and the global $\delta^{18}O$ record. *Science*, **313**, 492–495.
- Raymo, M.E. et al., 2011: Searching for Eustasy in Pliocene Sea-Level Records. *Nat. Geosci.*, **4**, 328–332, doi:10.1038/ngeo1118.
- Rogers, K.G. and I. Overeem, 2017: Doomed to drown? Sediment dynamics in the human-controlled floodplains of the active Bengal Delta. *Elementa Sci-Anthrop.*, **5**(66), doi:10.1525/elementa.250.
- Rohling, E.J. et al., 2014: Sea-level and deep-sea-temperature variability over the past 5.3 million years. *Nature*, **508**, 477, doi:10.1038/nature13230.
- Rolph, R.J., A.R. Mahoney, J. Walsh and P.A. Loring, 2018: Impacts of a lengthening open water season on Alaskan coastal communities: deriving locally relevant indices from large-scale datasets and community observations. *The Cryosphere*, **12**(5).
- Rovere, A. et al., 2014: The Mid-Pliocene sea-level conundrum: Glacial isostasy, eustasy and dynamic topography. *Earth Planet. Sci. Lett.*, **387**, 27–33, doi:10.1016/j.epsl.2013.10.030.
- Rovere, A. et al., 2016: The analysis of Last Interglacial (MIS 5e) relative sea-level indicators: Reconstructing sea-level in a warmer world. *Earth-Sci. Rev.*, **159**, 404–427, doi:10.1016/j.earscirev.2016.06.006.
- Schaefer, J.M. et al., 2016: Greenland was nearly ice-free for extended periods during the Pleistocene. *Nature*, **540**(7632), 252–255, doi:10.1038/nature20146.
- Schmidt, C.W., 2015: Delta subsidence: an imminent threat to coastal populations. *Environ. Health. Perspect.*, **123**(8).
- Schmitt, K., T. Albers, T. Pham and S. Dinh, 2013: Site-specific and integrated adaptation to climate change in the coastal mangrove zone of Soc Trang Province, Viet Nam. *J. Coast. Conserv.*, **17**(3), 545–558.
- Schmitt, R., Z. Rubin and G. Kondolf, 2017: Losing ground-scenarios of land loss as consequence of shifting sediment budgets in the Mekong Delta. *Geomorphology*, **294**, 58–69.
- Seroussi, H. and M. Morlighem, 2018: Representation of basal melting at the grounding line in ice flow models. *The Cryosphere*, **12**(10), 3085–3096, doi:10.5194/TC-12-3085-2018.
- Shakun, J.D. et al., 2018: Minimal East Antarctic Ice Sheet retreat onto land during the past eight million years. *Nature*, **558**(7709), 284–287, doi:10.1038/s41586-018-0155-6.
- Shammi, M. et al., 2017: Spatio-temporal assessment and trend analysis of surface water salinity in the coastal region of Bangladesh. *Environ. Sci. Pollut. Res.*, **24**(16), 14273–14290.
- Smajl, A. et al., 2015: Responding to rising sea levels in the Mekong Delta. *Nat. Clim. Change*, **5**(2), 167–174.
- Solomon, S.M., 2005: Spatial and temporal variability of shoreline change in the Beaufort-Mackenzie region, Northwest Territories, Canada. *Geo-Marine Letters*, **25**(2–3), 127–137.
- Stap, L.B. et al., 2016: CO2 over the past 5 million years: Continuous simulation and new 11B-based proxy data. *Earth Planet. Sci. Lett.*, **439**, 1–10, doi:10.1016/j.epsl.2016.01.022.
- Stap, L.B. et al., 2018: Modeled Influence of Land Ice and CO2 on Polar Amplification and Paleoclimate Sensitivity During the Past 5 Million Years. *Paleoceanogr. Paleoclimatol.*, **33**(4), 381–394, doi:10.1002/2017pa003313.
- Stone, E.J., D.J. Lunt, J.D. Annan and J.C. Hargreaves, 2013: Quantification of the Greenland ice sheet contribution to Last Interglacial sea level rise. *Clim. Past*, **9**(2), 621–639, doi:10.5194/cp-9-621-2013.
- Storlazzi, C. et al., 2018: Most atolls will be uninhabitable by the mid-21st century due to sea-level rise exacerbating wave-driven flooding. *Sci. Adv.* **4**(4), eaap9741.
- Sussman, F. et al., 2014: Climate change adaptation cost in the US: what do we know? *Climate Policy*, **14**(2), 242–282.
- Sutter, J. et al., 2016: Ocean temperature thresholds for Last Interglacial West Antarctic Ice Sheet collapse. *Geophys. Res. Lett.*, **43**(6), 2675–2682, doi:10.1002/2016GL067818.
- Szabo, S. et al., 2015: Scenarios of population change in the coastal Ganges Brahmaputra delta (2011–2051). *Asia-Pacific Population Journal*, **30**(2), 51–72.
- Takagi, H., N. Thao and L. Anh, 2016: Sea-level rise and land subsidence: impacts on flood projections for the Mekong Delta's largest city. *Sustainability*, **8**(9), 959.
- Terry, J.P. and T.F.M. Chui, 2012: Evaluating the fate of freshwater lenses on atoll islands after eustatic sea-level rise and cyclone-driven inundation: A modelling approach. *Global Planet. Change*, **88**, 76–84.

- Timsina, J. et al., 2018: Can Bangladesh produce enough cereals to meet future demand? *Agric. Syst.*, **163**, 36–44.
- Tran Anh, D., L. Hoang, M. Bui and P. Rutschmann, 2018: Simulating future flows and salinity intrusion using combined one-and two-dimensional hydrodynamic modelling – the case of Hau River, Vietnamese Mekong delta. *Water*, **10**(7), 897.
- Uddin, M.N. et al., 2019: Mapping of climate vulnerability of the coastal region of Bangladesh using principal component analysis. *Appl. Geogr.*, **102**, 47–57.
- UNDP, 2016: *Vietnam drought and saltwater intrusion: Transitioning from Emergency to Recovery. Analysis Report and Policy Implications*. United Nations Development Programme [Available at: [https://reliefweb.int/sites/reliefweb.int/files/resources/Recovery%20draft%20Sep%202016_final%20\(2\).pdf](https://reliefweb.int/sites/reliefweb.int/files/resources/Recovery%20draft%20Sep%202016_final%20(2).pdf)]. Accessed: 2019/09/20.
- Van Copenolle, R., C. Schwarz and S. Temmerman, 2018: Contribution of mangroves and salt marshes to nature-based mitigation of coastal flood risks in major deltas of the world. *Estuar. Coasts*, **41**(6), 1699–1711.
- Van Cuong, C., M. Russell, S. Brown and P. Dart, 2015: Using Shoreline Video Assessment for coastal planning and restoration in the context of climate change in Kien Giang, Vietnam. *Ocean Science Journal*, **50**(2), 413–432.
- Van Hoodonk, R., J. Maynard and S. Planes, 2013: Temporary refugia for coral reefs in a warming world. *Nat. Clim. Change*, **3**(5), 508.
- Vanderlinden, J.-P. et al., 2018: Scoping the risks associated with accelerated coastal permafrost thaw: lessons from Bykovsky (Sakha Republic, Russian Federation) and Tuktoyaktuk (Northwest Territories, Canada). In: *European Geosciences Union General Assembly*, Vienna, Austria, Geophysical Research Abstracts 20.
- Veettil, B.K. et al., 2018: Mangroves of Vietnam: Historical development, current state of research and future threats. *Estuar. Coast. Shelf Sci.* **218**, 212–236.
- Vellinga, P., 2009: *Exploring high-end climate change scenarios for flood protection of the Netherlands*. International Scientific Assessment, Netherlands [Available at: <http://bibliotheek.knmi.nl/knmipubWR/WR2009-05.pdf>]. Accessed: 2019/09/20.
- Vermaire, J.C. et al., 2013: Arctic climate warming and sea ice declines lead to increased storm surge activity. *Geophys. Res. Lett.*, **40**(7), 1386–1390.
- Vu, D., T. Yamada and H. Ishidaira, 2018: Assessing the impact of sea level rise due to climate change on seawater intrusion in Mekong Delta, Vietnam. *Water Sci. Technol.*, **77**(6), 1632–1639.
- Vyverberg, K. et al., 2018: Episodic reef growth in the granitic Seychelles during the Last Interglacial: Implications for polar ice sheet dynamics. *Mar. Geol.*, **399**, 170–187, doi:10.1016/j.margeo.2018.02.010.
- Wadey, M., S. Brown, R.J. Nicholls and I. Haigh, 2017: Coastal flooding in the Maldives: an assessment of historic events and their implications. *Nat. Hazards*, **89**(1), 131–159.
- Wang, Y. et al., 2015: Evolutionary History of Atmospheric CO₂ during the Late Cenozoic from Fossilized Metasequoia Needles. *PLoS ONE*, **10**(7), doi:10.1371/journal.pone.0130941.
- Warner, J.F., M.F. van Staveren and J. van Tatenhove, 2018: Cutting dikes, cutting ties? Reintroducing flood dynamics in coastal polders in Bangladesh and the Netherlands. *Int. J. Disast. Risk Reduc.*, **32**, 106–112.
- White, I. and T. Falkland, 2010: Management of freshwater lenses on small Pacific islands. *Hydrogeol. J.*, **18**(1), 227–246.
- Whitehead, P. et al., 2019: Water quality modelling of the Mekong River basin: Climate change and socioeconomics drive flow and nutrient flux changes to the Mekong Delta. *Sci. Total Environ.*, **673**, 218–229.
- Wilson, C.A. and S.L. Goodbred Jr, 2015: Construction and maintenance of the Ganges-Brahmaputra-Meghna delta: linking process, morphology, and stratigraphy. *Annu. Rev. Mar. Sci.*, **7**, 67–88.
- Winnick, M.J. and J.K. Caves, 2015: Oxygen isotope mass-balance constraints on Pliocene sea level and East Antarctic Ice Sheet stability. *Geology*, **43**(10), 879–882, doi:10.1130/G36999.1.
- Xian, S., J. Yin, N. Lin and M. Oppenheimer, 2018: Influence of risk factors and past events on flood resilience in coastal megacities: comparative analysis of NYC and Shanghai. *Sci. Total Environ.*, **610**, 1251–1261.
- Yamamoto, L. and M. Esteban, 2015: Adaptation strategies in deltas and their consequence on maritime baselines according to UNCLOS—the case of Bangladesh and Vietnam. *Ocean Coast. Manage.*, **111**, 25–33.
- Yamane, M. et al., 2015: Exposure age and ice-sheet model constraints on Pliocene East Antarctic ice sheet dynamics. *Nat. Commun.*, **6**, 7016, 1–8, doi:10.1038/ncomms8016.
- Yamano, H. et al., 2007: Atoll island vulnerability to flooding and inundation revealed by historical reconstruction: Fongafale Islet, Funafuti Atoll, Tuvalu. *Global Planet. Change*, **57**(3–4), 407–416.
- Yau, A.M., M. Bender, A. Robinson and E. Brook, 2016: Reconstructing the last interglacial at Summit, Greenland: Insights from GISP2. *PNAS*, **113**(35), 9710–9715, doi:10.1073/pnas.1524766113.
- Yu, H., E. Rignot, M. Morlighem and H. Seroussi, 2017: Iceberg calving of Thwaites Glacier, West Antarctica: full-Stokes modeling combined with linear elastic fracture mechanics. *The Cryosphere*, **11**(3), 1283–1296.
- Zhang, Y.G. et al., 2013: A 40-million-year history of atmospheric CO₂. *Phil. Trans. R. Soc. A*, **371**(2001), 20130096.
- Zhou, Z., S. Liu, G. Zhong and Y. Cai, 2016: Flood disaster and flood control measurements in Shanghai. *Natural Haz. Rev.*, **18**(1), B5016001.
- Zoccarato, C., P.S. Minderhoud and P. Teatini, 2018: The role of sedimentation and natural compaction in a prograding delta: insights from the mega Mekong delta, Vietnam. *Sci. Rep.*, **8**(1), 11437.